2011

Evaluating the duration of post-LGM grounding events in the Glomar Challenger Basin paleotrough, Eastern Basin Antarctica, using sediment flux calculations

Boluwatife Owolana
Louisiana State University and Agricultural and Mechanical College

EVALUATING THE DURATION OF POST-LGM GROUNDING EVENTS IN THE GLOMAR CHALLENGER BASIN PALEOTROUGH, EASTERN BASIN ANTARCTICA, USING SEDIMENT FLUX CALCULATIONS

A Thesis

Submitted to the Graduate Facility of

Louisiana State University and

Agricultural and Mechanical College

in the partial fulfillment of the

requirements for the degree of

Master in Science

in

The Department of Geology and Geophysics

by

Boluwatife Owolana

B.S., Neumann University, 2007

December 2011

Dedication

I dedicate this to my parents, Dr. & Mrs. Owolana. Without their unending love, guidance, advice and support over the years, I wouldn't be where I am today.

Acknowledgements

I would like to acknowledge my advisor, Dr. Philip Bart, for all his guidance and advice throughout the length of my graduate education at LSU. I'd like to thank my committee members Dr. Brooks Ellwood, Dr. Sam Bentley for all their input in conducting this research and writing of this thesis. Thanks to Dr. Juan Lorenzo and Dr. Ruixia Xu for their help with Seismic Unix. I'd also like to thank the LSU Department of Geology and Geophysics for supporting me financially for two years as a Teaching Assistant. Additional financial support was also provided by Devon Energy through a scholarship. Special thanks to my colleagues and friends who have assisted me in various ways during the pursuit of my Master's degree here at LSU. Also to the LSU golf course for providing times of relaxation.

Thanks to John Anderson and German Leitchenkov for access to seismic data they acquired during PD90, NBP94, NBP95 and M89. The members of the NBP0802-03 expedition (Edison Chouset ship crew and Raytheon Polar Services support) assisted the geophysical and geological data acquisition.

Table of Contents

List of Tables

List of Figures

Abstract

Previously acquired geological and geophysical data from the eastern Ross Sea outer shelf support the view that the West Antarctic Ice Sheet (WAIS) deposited three large-volume grounding zone wedges (GZWs) during the relatively short time since the onset of ice sheet retreat began at approximately 11 ka ^{14}C BP. Here, GZW sediment volumes were estimated from seismic data correlations to evaluate the different possible durations of the individual grounding events. The two end-member fluxes used correspond to 1) a modern flux active at Whillans Ice Stream and 2) a larger flux accounting for the larger size of the drainage basin at LGM. Two basic experiments were conducted. In the first experiment, calculations of grounding-event durations were based on 2D estimates of GZW volumes from a regional dip-oriented seismic transect. The second experiment focused on 3D-volume estimates for the youngest GZW on middle shelf, which is referred to as the Gray Unit. The 3D volume of the Gray Unit was used to calculate Gray Unit grounding-event duration. The results from the 2D experiment are invalid for this study because the analysis showed that the study requires a 3D approach. The grounding-event durations calculated for the 3D experiment suggests that the three GZWs could not have been deposited within the short time elapsed since the onset of post-LGM ice-sheet retreat. Instead, the long duration needed to deposit the Gray-Unit GZW favors the alternate view that each wedge was deposited during at least part of the advance phase of the last glacial cycle. Following this line of reasoning suggests that Gray Unit GZW corresponds to deposition beginning in OIS 3 and ending during OIS 2 i.e. the last glacial maxima, whereas the older GZWs must represent deposition during successively older pre-LGM glacial maxima.

Introduction

Much geological and geophysical data strongly support the view that the Antarctic Ice Sheet advanced to the outer shelf during the last glacial maximum (LGM) (e.g., Conway et al., 1999; Shipp et al., 1999; Bentley et al., 1999). It is also generally accepted that the retreat from the outer shelf involved a series of pauses followed by liftoff retreats (Conway et al., 1999; Domack et al., 1999; Mosola and Anderson, 2006). The last decoupling retreat led to the establishment of the current grounding line positions on the inner continental shelves (Figure 1). The current grounding event is thought to have lasted a millennium (Anandrakrishnan et al., 2007). High-resolution seismic surveys show that a series of subaqueous moraines referred to as grounding zone wedges (GZWs), occupy the axes of paleotroughs on the outer shelf. These GZWs represent deposition at the terminus of grounded ice during a pause in the overall retreat. Indeed, the seafloor morphology and the near-surface stratal patterns are consistent with the view of backstepping retreat in several steps. In the eastern Ross Sea, the West Antarctic Ice Sheet (WAIS) paused three times on the outer and middle shelf in the Glomar-Challenger-Basin (Mosola and Anderson, 2006) (Figure 2). The Glomar-Challenger-Basin is a major cross-shelf paleotrough that can be traced southward below the Ross Ice Shelf as a bathymetric feature to the mouth of the Whillans Ice Stream (Bart, 2004).

The stratigraphy is of interest because it affords the opportunity to precisely date the onset and termination of multiple liftoff retreats. Unfortunately, the actual chronology of individual retreats has proven difficult to establish for the outer shelf. Most radiocarbon data indicate that open-marine sedimentation was occurring by 11 ka ^{14}C BP and this is taken to represent ice sheet retreat in association with rapid climate warming and sea level rise during the transition from OIS 2 to OIS 1 (Domack et al., 1999). With respect to dating individual liftoff events, the lack of progress is due to a paucity of datable material and the problem of distinguishing between *in situ* and recycled material within the glacial setting (Andrew et al., 1999). In a major synthesis of onshore and offshore data, Conway et al. (1999) proposed that grounded ice had completely vacated the eastern Ross Sea shelf by 7.8 ka ^{14}C BP. Modeling of radar reflection data at the Roosevelt Bank ice rise on the Ross Ice Shelf (Figure 1) is consistent with this interpretation, suggesting that grounded ice continued its retreat to the inner shelf pass Roosevelt Island by approximately 3.2 ka ^{14}C BP (Conway et al., 1999). In this view, all three post-LGM GZWs on the outer and middle shelf sectors of the Glomar-Challenger-Basin were deposited during a relatively short 3.2 kyr timeframe, i.e., after 11 ka ^{14}C BP and before 7.8 ka ^{14}C BP.

This scenario is potentially problematic because it requires that large volumes of GZW sediment were deposited within a short amount of time. Bart and Cone (2011) proposed an alternate interpretation of the near surface stratigraphy. In their view, the middle shelf GZW, the youngest GZW in the Glomar-Challenger-Basin represents deposition during the LGM (Figure 2). This conclusion is based on dating of *in situ* forams isolated from the foreset surface of the middle shelf GZW. This middle shelf GZW unit is referred to as the Gray Unit (Bart, 2004). The older GZWs on the outer continental shelf of the Glomar Challenger Basin were referred to as the Brown-, Red-, and Purple-Unit GZWs (Figures 2 and 3B) (Bart, 2004). If the Gray GZW is assigned to the LGM, then the Brown-, Red- and Purple-Unit GZWs (Figure 3B), may correspond to

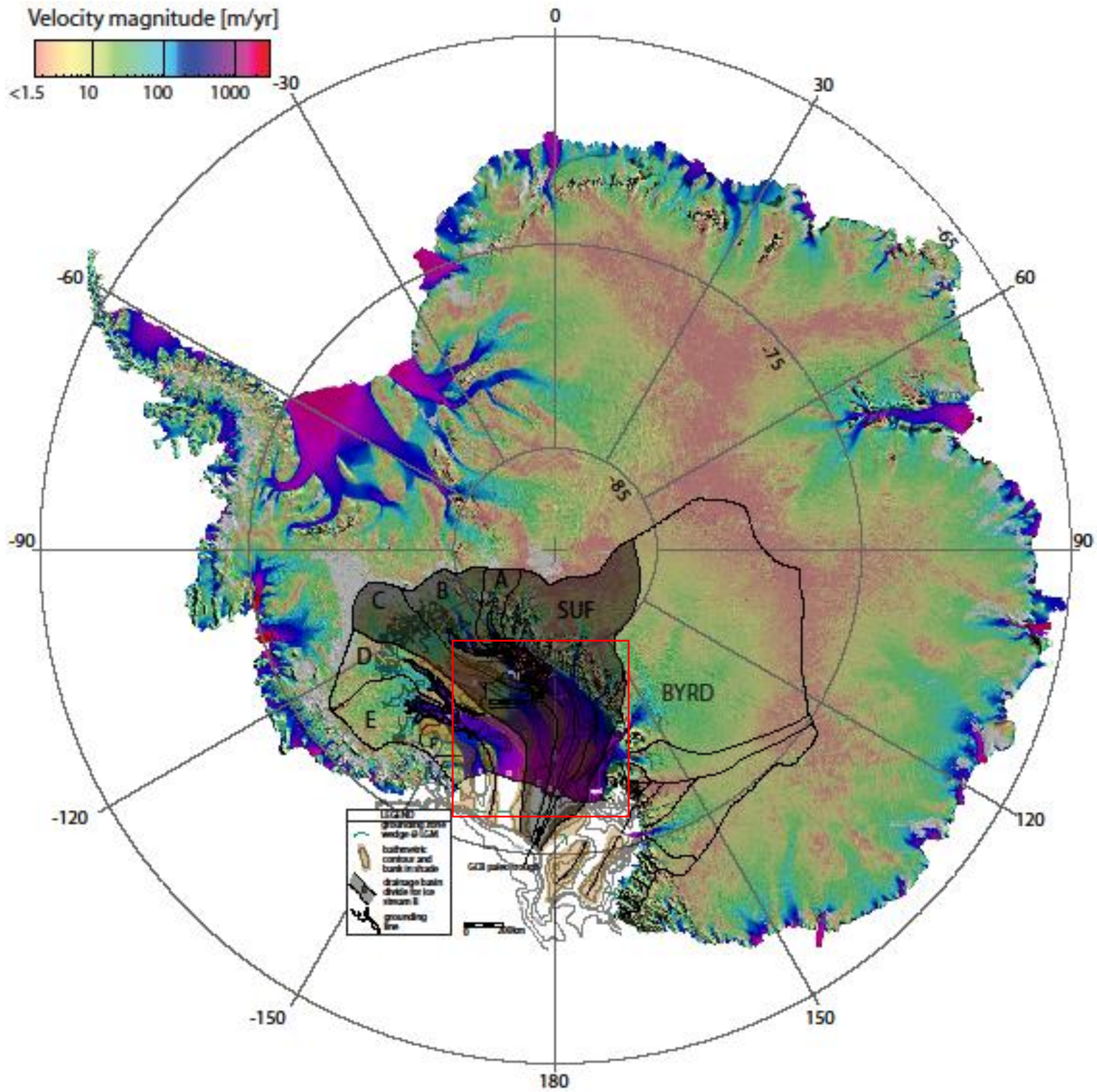

Figure 1. Map of Antarctica showing the ice velocity flow and drainage basin boundaries from Rignot et al. (2011). Dashed black lines around B indicate drainage area for the Whillans Ice Stream, the shaded area indicate the drainage area for the Glomar-Challenger-Basin at LGM, and the solid black line indicate the LGM drainage area. The red box shows the location of eastern Ross Sea shown in Figure 2.

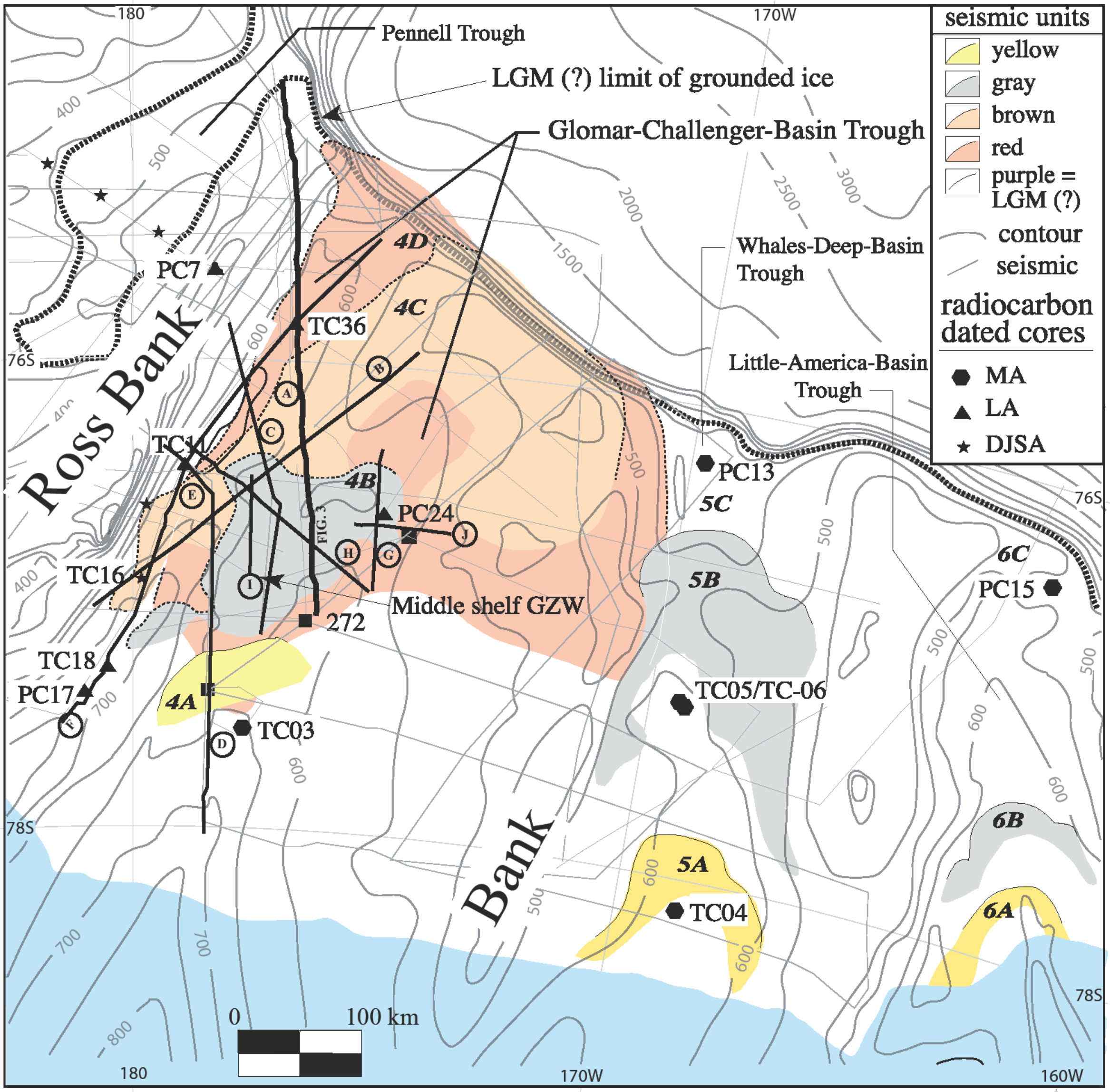

Figure 2. Eastern Ross Sea basemap showing the location of Glomar-Challenger-Basin, a paleotrough. The Red, Brown and Gray shaded regions show the surface locations of grounding zone wedges exposed at the seafloor based on information from Bart (2004). The four units are assigned to the LGM and post-LGM by Mosola and Anderson (2006). The heavy black lines show the location of seismic data shown in Figure 3. The heavy lines marked A-J correspond to seismic lines shown in Figure 4.

three discrete glacial maxima prior to LGM (i.e., OIS 4, OIS 6, OIS 8, and OIS 10). Following this line of reasoning would suggest that the older GZWs are of considerable antiquity and took considerably more elapsed time than the post-LGM interpretation affords. These two interpretations of how the near-surface stratigraphy relate to translations of the WAIS grounding line are obviously incompatible.

Given the problems of distinguishing *in situ* from recycled carbon, a different strategy was used to evaluate these two interpretations of how GZWs stratigraphy in the Glomar Challenger Basin relates to WAIS glacial history (Domack et al., 1999; Bart and Cone, 2011). The objective of this study was to use two end-member sediment flux values based on recent estimates of modern flux at the Whillans Ice Stream (Anandrakrishnan et al., 2007) to evaluate a range of grounding event durations. If the GZWs in the Glomar Challenger Basin were deposited following the onset of post-LGM retreat at 11 ka ^{14}C BP, then the cumulative durations of all three grounding events, the Red, Brown and Gray GZWs, should be less than 3200 years. Conversely, if the three GZWs represent deposition during three discrete glacial maxima (i.e., OIS 2, OIS 4, OIS 6, and OIS 8), then the durations for each wedge may range from ~20 kyr to 100 kyr durations.

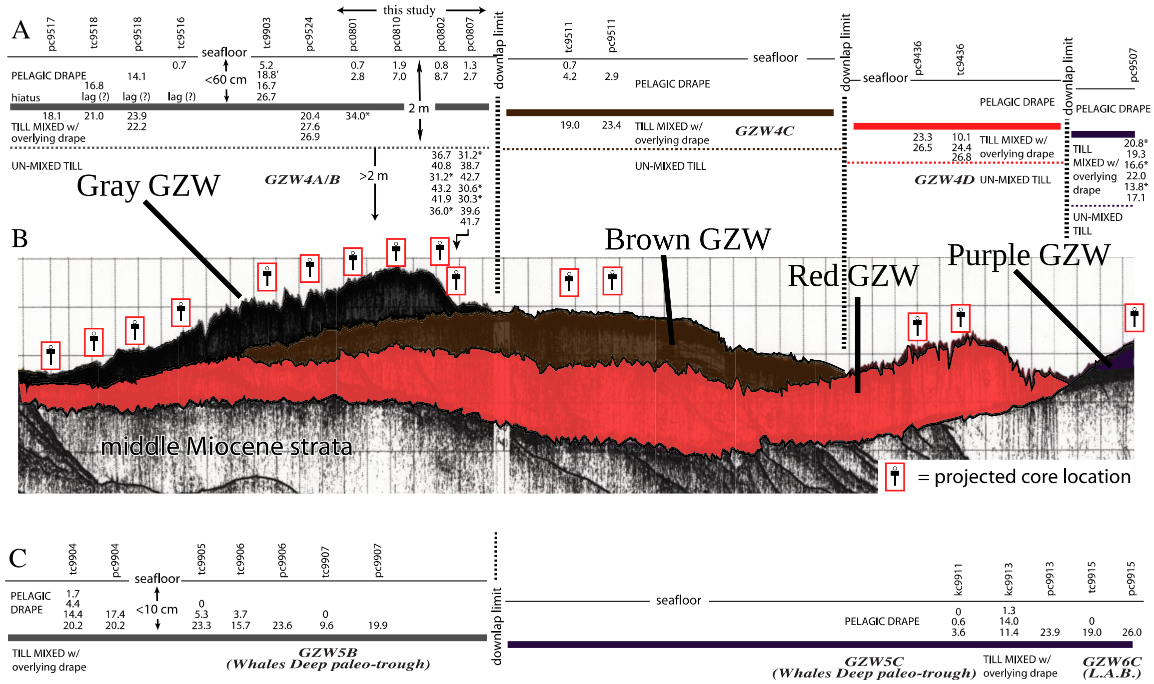

Figure 3. Interpretation of regional dip-oriented single-channel seismic line M89-27 in the axis of Glomar-Challenger-Basin (see Figure 2 for the map location of the transect) from Bart and Cone (2011). The Purple Unit represents a grounding zone wedge (GZW) assigned to the LGM (Shipp et al., 1999; Mosola and Anderson, 2006). The overlying Red, Brown and Gray Units were interpreted by Mosola and Anderson (2006) to represent a series of GZWs exhibiting an overall backstepping retreat of the West Antarctic Ice Sheet. According to Domack et al. (1999) WAIS retreat from Ross Sea began at ~11 kyr ^{14}C BP. In an alternate interpretation, Bart and Cone (2011) propose that the Gray Unit represents deposits associated with the LGM advance of the WAIS. In their view, each of the older GZWs represents discrete glacial cycles (Bart and Cone, 2011).

Background

Modern Sediment Flux at the Whillans Ice Stream in Grounding Zone Wedge

At Whillans Ice Stream, the modern flux is reported as 200 m^3/m/a (Anandrakrishnan et al., 2007). This is the standard way in which flux is reported but in this case, the flux is not based on a 3D evaluation of the GZW volume. For this reason, the flux from Anandakrishnan et al. (2007) is hereafter referred to as a 2D flux by Anandakrishnan et al. (2007). This modern 2D flux estimate is based on a single 2D radar image showing the volume of the modern GZW actively accumulating at the mouth of Whillans Ice Stream (Figure 1). The usefulness of this modern 2D flux for this study depends on the veracity of the two following tacit assumptions. Firstly, it is assumed that the Whillans GZW was deposited within 1000 years. Secondly, it is assumed that the GZW is a line sourced feature, i.e., cross-sectional area observed on any 2D radar image is representative of the GZW's average volume per meter width of the grounding line. Given that flux is defined as the quantity of sediment exiting the drainage basin per unit of time, the actual (i.e., 3D) flux for Whillans Ice Stream is calculated using Equation 1 below.

$$\text{3D Flux } (m^3/a) = \text{2D Flux } (m^3/m/a) \times \text{Ice Stream width at the grounding line } (m) \qquad (1)$$

Upstream of the grounding line, the Whillans Ice Stream width is 30 kilometers (Truffer and Echelmeyer, 2003) but recent data (Rignot et al., 2011) show that the ice stream merges with Ice Stream A and widens to 200 kilometers at the grounding line. Therefore, for example, if the downstream GZW is taken to be 30 km wide, then the actual (3D) modern flux would be 6.0×10^6 m^3/a (i.e., 30 km x 200 m^3/m/a). For these modern fluxes to be accurate, the active GZW at Whillans would have to be a line-source feature with cross-section slice volume similar to that measured by Anandakrishnan et al. (2007) along a 30 km or 200 km width dimension of the Whillans Ice Stream. The modern flux from Anandakrishnan et al. (2007) would also be in error by some unknown amount if the Whillans GZW took considerably longer or shorter than 1000 years to construct. For example, if the Whillans GZW took 2000 years to construct, then the modern fluxes would be slower by one-half. Obviously, caution should be exercised when using the modern flux estimates. Until further data is available and for the purposes of this experiment, it is accepted that the modern GZW at Whillans was constructed over a 1000 year time interval and that the GZW is a simple line source. Given this range of modern fluxes (6.0×10^6 m^3/a to 4.0×10^7 m^3/a) and dimension of the Whillans Ice Stream drainage basin[1] (235200 km^2; Rignot et al., 2002), a yield (in $m^3/m^2/a$) can be calculated using Equation 2.

$$\text{Yield } (m^3/m^2/a) = \text{Flux } (m^3/a) \,/\, \text{Drainage Area } (m^2) \qquad (2)$$

Using this range of modern constraints, the yield from the Whillans Ice Stream drainage area would range from a minimum of 2.55×10^{-5} $m^3/m^2/a$ to a maximum of 1.7×10^{-4} $m^3/m^2/a$.

At the LGM, the Whillans Ice Stream occupied the Glomar-Challenger-Basin on the eastern Ross Sea outer shelf as inferred from bathymetric data (Bentley and Jezek, 1981). Thus, the drainage basin for the Whillans Ice Stream at LGM thus was significantly larger (Figure 1). The range of yields estimated for Whillans drainage

[1] Rignot et al. (2002) report the drainage area for the Whillans and Ice Stream A as a single value.

system in the modern were used for estimating the flux for the larger drainage basin that existed at the LGM. Data from Denton et al. (2000) show that the LGM drainage basin for the Whillans ice stream included a larger area of West Antarctica and a significant area of East Antarctica (Table 1). However, recent data from Licht et al. (2002) showed that the Byrd glacier drainage basin delivered ice and sediment to western and central Ross Sea i.e., not to the Glomar-Challenger-Basin paleotrough. The yield from the additional West Antarctic sector was probably similar to the yield calculated for the modern Whillans Ice Stream. In contrast, basement rock on the East Antarctica drainage basin sector may have liberated a lower yield (Schlunegger et al., 2001). Given that the drainage basin was significantly larger, then the LGM flux should have been higher.

Table 1. Drainage areas for East and West Antarctica from Rignot et al. (2002). The modern drainage area for the "Whillans" GZW corresponds to A&B. During the LGM, the GCB drainage area included the areas shaded plus the offshore area shown in Figure 1. GZW = Grounding Zone Wedge. GCB = Glomar Challenger Basin. LGM = Last Glacial Maximum

MAP SYMBOL	Drainage basin areas
A & B	2.352×10^{11} m^2
C	1.534×10^{11} m^2
D	1.403×10^{11} m^2
E	1.752×10^{11} m^2
F	1.68×10^{10} m^2
SUF	2.352×10^{11} m^2
BYRD	1.07×10^{12} m^2
OFFSHORE	3.867×10^{11} m^2

Methods

The stratigraphy of the Glomar-Challenger-Basin paleotrough was the focus of this study because the GZWs assigned to LGM and the post-LGM have been well mapped in previous studies using seismic and multibeam data (Bart et al., 2004; Mosola and Anderson, 2006; Bart and Cone, 2011). Bart (2004) referred to the unit assigned to the LGM as the Purple Unit, whereas the younger units assigned to the post-LGM timeframe are referred to as the Red, Brown and Gray units. Each unit is taken to be a discrete depositional episode, i.e., a grounding event that constructed a GZW.

Two basic experiments were conducted to estimate the duration of the grounding events associated with the deposition of the Purple, Red, Brown and Gray GZWs. The first experiments involved a 2D evaluation of the 3 GZWs in Glomar Challenger Basin. The estimated durations were calculated from seismic based estimates of the GZW volume and recent measurements of modern flux at the Whillans-Ice-Stream GZW. The calculation used the relationship between flux, GZW volume and duration shown in Equation 3.

$$d = v_s \; / \; F \qquad (3)$$

where v_s is sediment volume (m^3/m), F is the flux rate ($m^3/m/a$) and d is duration in years (a). The durations calculated in the second experiment were based on a 3D approach to estimate the volume for only the Gray Unit GZW on the middle shelf, i.e., the youngest of three GZWs assigned to the post-LGM timeframe. In both cases, it is assumed that all flux was sequestered in the GZW as traction mode. This assumption is consistent with modern observations showing that no significant melt-water plumes exist in the current dry Antarctic polar climate (Anderson, 1999). Given this constraint, it is improbable that copious melt water existed during the colder LGM. For both the 2D and 3D approaches, grounding event durations using a range of estimates for modern flux (Anandakrishnan et al., 2007) was first calculated and a second range of larger flux estimates to account for a larger drainage basin existing at LGM.

2D Approach to Estimating GZW Durations

In the 2D experiment, the time needed to deposit the GZW assigned to LGM and the three GZWs assigned to the post LGM using a single regional seismic transect was estimated. The premise of this approach is that the GZW is a line source feature so that any dip oriented cross section is representative of the units' total sediment volume. The seismic line used to measure the GZWs' length and thickness was a dip-oriented profile; line M89-27, located near the axis of the Glomar-Challenger-Basin paleotrough (Figure 3). Line M89-27 was selected because it shows the stratigraphic arrangement of the LGM unit and all three post-LGM GZW units (Purple, Red, Brown, and Gray GZWs) on a single transect. Mosola and Anderson (2006) referred to the Red, Brown and Gray units as GZW4D, GZW4C, and GZW 4B respectively (Figure 2).

To calculate the seismic cross-section area of the Purple, Red, Brown, and Gray GZWs, seismic line M89-27 was scanned and saved in TIFF format using a HP Designjet wide format scanner. The resulting TIFF file was then imported into Didger®, and digitized to calculate the cross-section area of the GZW units. To accurately digitize and calculate the areas, the vertical axes in two-way travel time (TWTT), and horizontal axes of the seismic line were converted into units of depth and length, respectively. The

TWTT was converted into depth by using a range of velocities (1500, 1750, 2000 and 2250 m/s) using Equation 4 below:

$$D = vt / 2 \tag{4}$$

where D is the depth (in meters), v is the sediment velocity (in m/s), and t is the two-way travel time (s).

Horizontal distance was determined from the navigation base map for line M89-27 (Figure 3). Navigation point 8700 on the seismic line is at longitude 182° 44.1600' W and latitude 76° S. Navigation point 900 is at longitude 183° 13.20000' and latitude W, 77° S. The distance between these two points was calculated to be 113.7 km. There are 21 equi-distant time-stamped shot points between point 8700 and 900, therefore by interpolation, the distance between each navigation point is calculated by dividing 113.7 km by the 21 points, and thus is equal to 5.4 km.

With the newly calculated coordinate system, the TIFF version of seismic line M89-27 was imported into Didger® and three calibration points were selected; an origin, a point on the x-axis, and a third point on the y-axis. The outline of each GZW was digitized, and Didger® software was used to calculate the cross-section area.

The 2D cross-section areas of the GZWs were converted to a 2D-slice volume by assuming that the 2D area was consistent over a 1-meter width of the grounding line. Mapping results presented by Bart (2004) suggest that the cross-section areas observed on seismic line M89-27 are a reasonable representation of the average GZW volume along the entire 140 km strike-oriented width of the Glomar-Challenger-Basin paleotrough. In other words, the assumption was made that the relationship between actual 3D volumes, 2D cross-section slice volume at line M89-27, and the GZW width is defined as soon in Equation 5.

$$3D\ \text{Volume}\ (m^3) = 2D\ \text{Cross Section volume}\ (m^3/m) \times \text{GZW width}\ (m) \tag{5}$$

This relationship however does not apply to the Purple GZW, the unit assigned to the LGM, because M89-27 crosses the Purple unit on the flank of the Glomar-Challenger-Basin at Ross Bank (Figure 2). At this location, the unit is relatively narrow and thin whereas regional mapping shows that the Purple GZW is considerably thicker in the axis and eastern flank of the Glomar-Challenger-Basin (Bart, 2004).

With the 2D-volume estimates, the duration of the GZW grounding events were calculated using a modern 2D flux and LGM 2D fluxes for the Glomar-Challenger-Basin paleo ice stream. The modern 2D flux used was the same as that reported by Anandrakrishnan et al. (2007). The grounding-event durations for each GZW was calculated from the computed 2D slice volume using Equation 3. LGM reconstructions suggest that the drainage basin for the Glomar Challenger Basin was significantly larger during the LGM (Figure 1; Table 1). Thus, the modern flux should under-estimate the durations of the GZW on the outer shelf. The LGM drainage basin for the Glomar Challenger Basin included additional parts of West Antarctica and some sectors of East Antarctica. Thus, the flux from West Antarctica and East Antarctica need to be combined. In this study, it was assumed that the yield from all West Antarctic sections of the LGM drainage basin were the same as that which was inferred for the modern Whillans-Ice-Stream drainage area. The product of the modern yield times the larger

LGM drainage basin configuration for West Antarctica (Equation 2) was used to calculate the LGM flux contribution from West Antarctica.

Data presented by Schlunegger et al. (2001) suggest that yield depends on rock type. Given the East Antarctic is underlain by basement rock, it was assumed that yield from East Antarctica was 30% less than that for sedimentary strata underlying West Antarctica. Therefore, an East Antarctic yield was calculated using Equation 6.

$$\text{West Antarctic Yield } (Y_{WA}) = 0.7 \text{ x East Antarctic Yield } (Y_{EA}) \qquad (6)$$

The product of the East-Antarctic yield times the East Antarctic part of the LGM drainage basin was used to calculate a LGM flux for the East Antarctic sectors providing flux to the Glomar-Challenger-Basin paleo trough (Equation 2). The cumulative LGM flux was therefore the sum of flux contributions from West Antarctica and East Antarctica. This (3D) LGM flux was divided by the 140 km width of the Glomar-Challenger-Basin paleo ice stream (Figure 2) to generate a range of 2D LGM flux in m^3/m/a (Equation 4). The ranges of fluxes were based on 30-km, 100-km, and 200-km widths of the Whillans Ice Stream. These 2D LGM fluxes were used to calculate grounding event durations from 2D sediment volumes as measured on line M89-27 using Equation 5. If the three GZWs were deposited within the post-LGM timeframe, then the duration should be less than 3200 years, i.e., the time elapsed between 11 and 7.8 ka ^{14}C BP.

3D Approach to Estimating the Middle-Shelf Grounding Event Duration

The 3D experiment was focused on the Gray GZW on the middle continental shelf. In this experiment, the grounding event duration was based on a 3D assessment of the Gray-GZW sediment volume. To calculate the volume of the Gray GZW, the top and base of the Gray unit was correlated on seismic data from six single-channel seismic surveys, M89, PD90, NBP94, NBP95, NBP03, and NBP08. M89 was acquired with a sparker source. PD and NBP data were acquired with a generator injector airgun source. The multibeam survey acquired in NBP08 was also used to more precisely define the limits of the Gray GZW in map view. The top and base of the Gray GZW were contour mapped. The isopach thickness in (milliseconds) of the Gray GZW was generated in Petrel® by subtracting TWTT ranges from the top and base of the Gray GZW. The isopach thickness in milliseconds was converted to sediment thickness in meters using a sediment velocity of 1750m/s. The volume was calculated by using the map extent of the Gray Unit (from the isopach map) multiplied by the average thickness for the Gray Unit, which was estimated using Petrel® interpretation software.

The grounding-event duration for the Gray Unit 3D volume was calculated using a range of flux rates corresponding to estimates of modern 3D fluxes and LGM 3D fluxes. The 3D modern flux rates are based on the modification of the modern 2D flux reported for Whillans Ice Stream (Anandakrishnan et al., 2007). The 3D modern fluxes are the products of the modern 2D flux (200 m^3/m/a) and the Whillans Ice Stream widths of 30 km, 100 km, and 200 km respectively (Equation 1).

The LGM 3D fluxes were used to account for the larger drainage basin that existed during LGM. As discussed in the previous section, the LGM flux is the sum of the larger LGM fluxes from East Antarctica and West Antarctica. The combined LGM flux from East Antarctica and West Antarctica based on varying widths of the Whillans Ice Stream (Table 2) was used to estimate the duration of the Gray GZW. If the Gray

GZW was deposited during the third pause of the WAIS during its overall post-LGM retreat, then it was arbitrarily assumed that its duration should be approximately 1000 years, i.e., approximately one-third of the 3.2 kyr post-LGM timeframe inferred for grounded ice to vacate Glomar Challenger Basin. Conversely, if the Gray GZW represents the culmination of erosion and deposition during the advance phase of the last glacial cycle e.g., from OIS 5 or OIS 4 to OIS 2, then the Gray GZW duration might be on the order of 100 kyr to 20 kyr respectively.

Table 2. Fluxes and annotated yields calculated for East and West Antarctica using minimum, intermediate and maximum estimates of Whillans Ice Stream

	FLUX			YIELDS		
	Whillans Ice Stream Width			Yields		
	Minimum (30km)	Intermediate (100 km)	Maximum (200 km)	Minimum (30km)	Intermediate (100 km)	Maximum (200 km)
East Antarctica	4.2×10^6 m^3/a	1.4×10^7 m^3/a	2.8×10^7 m^3/a	1.79×10^{-5} $m^3/m^2/a$	5.95×10^{-5} $m^3/m^2/a$	1.19×10^{-4} $m^3/m^2/a$
West Antarctica	1.98×10^7 m^3/a	6.59×10^7 m^3/a	1.32×10^8 m^3/a	2.55×10^{-5} $m^3/m^2/a$	8.5×10^{-5} $m^3/m^2/a$	1.70×10^{-4} $m^3/m^2/a$
Total cumulative Flux	2.4×10^7 m^3/a	8.0×10^7 m^3/a	1.6×10^8 m^3/a			

Results

2D Evaluation of GZW Volumes and Durations

The cross-section slice volumes for the outer shelf GZWs at dip-oriented seismic line M89-27 (Figure 3) were calculated (in m^3/m) using a range of sediment velocity estimates (Table 3). The cross-section slice volumes on the outer shelf contain significantly more volume than the slice volume measured for the modern GZW at the mouth of Whillans Ice Stream (Anandakrishnan et al., 2007). On the shelf, a comparison of the cross section volumes shows that the Gray- and Brown-Unit GZW volumes are similar whereas the Red-Unit GZW is significantly larger (Table 3). The grounding-event durations shown in Table 4 corresponds to the GZW volumes calculated using time-depth conversion based on an average sediment velocity of 1750 m/s (Table 3 column B). If a higher (lower) sediment velocity were used to make the time-depth conversion, then the estimated duration of the grounding events would be longer (shorter). The first set of grounding event durations shown in Table 4 (column B) represents the time elapsed to deposit the volume observed on line M89-27 using the modern 2D flux (200 m^3/m). Thus, if the 3 outer shelf GZW slices were deposited at flux rates comparable to the flux currently inferred to be existing at the Whillans ice stream (Anandakrishnan et al., 2007), then it would have taken a total of 65.6 kyr (11.5, 10.9, and 43.2 kyr) to deposit these 3 GZWs. The time elapsed for the deposition of the Purple GZW slice is estimated to have been 21.5 kyr

Grounding-event durations in Table 4 (column C corresponds to time intervals that would have elapsed to deposit the volumes observed on line M89-27 using the inferred minimum, intermediate, and maximum LGM 2D fluxes (see Methods). Using these values for LGM 2D fluxes, the Red, Brown and Gray GZWs would have taken elapsed times of 77, 23.1 and 11.5 kyr respectively to deposit.

The third set of grounding-event durations in Table 4 (column D) shows grounding event durations that would have occurred if the flux at the outer shelf were equal to 4102.2 m^3/m/a. This is the minimum flux that would have been required for the three GZWs to have been deposited within the 3200 years. This minimum required flux is ~20 times larger than the modern flux and ~3.5 times larger than the maximum LGM 2D flux.

Table 3. 2D volumes (m^3) per meter width of each GZW using different sediment velocity estimates from seismic line M89-27.

GZW Name	Slice Volume			
	T-D Velocity			
	A 1500 m/s	**B** 1750 m/s	**C** 2000 m/s	**D** 2250 m/s
Gray	1.931×10^6 m^3	2.304×10^6 m^3	2.634×10^6 m^3	2.963×10^6 m^3
Brown	1.824×10^6 m^3	2.176×10^6 m^3	2.487×10^6 m^3	2.798×10^6 m^3
Red	7.247×10^6 m^3	8.647×10^6 m^3	9.882×10^6 m^3	11.117×10^6 m^3
Purple	3.611×10^6 m^3	4.308×10^6 m^3	4.924×10^6 m^3	5.539×10^6 m^3

3D evaluation of GZW Volumes and Durations

Seismic profiles of the Gray-Unit GZW show that the feature has low-amplitude relief confined to the middle shelf of the Glomar-Challenger-Basin (Figure 4). The multibeam survey on the middle continental shelf sector of the Glomar Challenger Basin

Table 4. Grounding event durations of each GZW from 2D volume measured on seismic line M89-27 based on 2D modern flux and minimum required flux.

	A. GZW Slice Volume (m^3/m) based on a T-D conversion velocity of 1750 m/s (Table 4 Column B)	**B.** Durations using 2D modern flux (200 $m^3/m/yr$) (kyr)	**C.** Durations using 2D LGM Flux (kyr)			**D.** Duration using Minimum required flux (4102.2 $m^3/m/yr$) (kyr)
			Min (30 km)	Int (100 km)	Max (200 km)	
			171.2 $m^3/m/yr$	570.7 $m^3/m/yr$	1141.8 $m^3/m/yr$	
Gray	2.304 x 10^6	11.52	13.4	4.0	2.0	0.56
Brown	2.176 x 10^6	10.88	12.8	3.9	1.9	0.53
Red	8.647 x 10^6	43.24	50.8	15.2	7.6	2.1
TOTAL	**1.313 x 10^7**	**65.64**	**77**	**23.1**	**11.5**	**3.19**
Purple	4.308 x 10^6	21.54	25.1	7.5	3.8	1.05

also shows that the GZW is manifest as a low-relief feature on the middle shelf (Figure 5). The Gray GZW's upper surface is foredeepened. The deepest part of the GZWs' upper surface extends to 650 meter water depth whereas its shallowest upper surface is at a water depth of 500 meters. At the seaward termination of the Gray Unit, the multibeam data demonstrates that the Gray GZW has two lobes (Figure 5), i.e., the wedge is not a line source feature. The map view sinuosity of the lobe crest has an amplitude of 20 kilometers. Only part of the eastern lobe is imaged on the multibeam survey but its extent is confirmed with seismic data (Figures 2, 4J, and5). The top of the Gray GZW has well defined Mega Scale Glacial Lineations (MSGLs) and other features generally dip-aligned with the axis of the Glomar Challenger Basin that probably represent deep iceberg gouges (Figure 8). The heights of these features range from 1 meter to 24 meters.

These data show that iceberg keels reached depths in excess of 550 meters present-day water depth. The MSGLs can be followed northward to the dashed red line (Figure 7b), which defines the edge of the Gray GZW topset surface. The dashed line thus represents the limit of grounded ice at the end of the Gray Unit grounding event. The seafloor topography up to the solid line thus corresponds to the basal topography of the WAIS in the Glomar Challenger Basin prior to liftoff retreat. Immediately seaward of the Gray GZW topset, a narrow zone without MSGL dips seaward at a 0.5^{o} (Figure 6B). The absence of lineations on this surface shows that the seaward dipping surface corresponds to the GZW's foreset surface that was constructed in open water and was not overrun by grounded ice. Small-scale lobes of the foreset surface suggest that sedimentation at the grounding line may have been by the extrusion of relatively cohesive sediment (see inset of Figure 5). The pinchout of the Gray GZW occurs less than 5 km northward of the Gray Unit topset boundary (Figure 5).

The maximum height of the Gray GZW foreset surface is 50 meters (Figure 6C). The Gray Unit GZW partially buries the MSGL formed on the top of the Brown Unit GZW. The orientations of MSGLs on the top of the Brown Unit GZW are noticeably oblique to the orientation of MSGLs on top of the Gray Unit GZW (Figure 5 inset). A short distance basinward of the Gray GZW downlap limit, the MSGLs of the Brown Unit GZW are not buried at the seafloor indicating that most of the sediment reaching the Gray GZW foreset were deposited as traction mode sediment. In summary, cross sections of the seafloor based on the multibeam data clearly show a well-defined foreset, topset and bottomset geometry associated with a thick and broad Gray GZW (Figure 6).

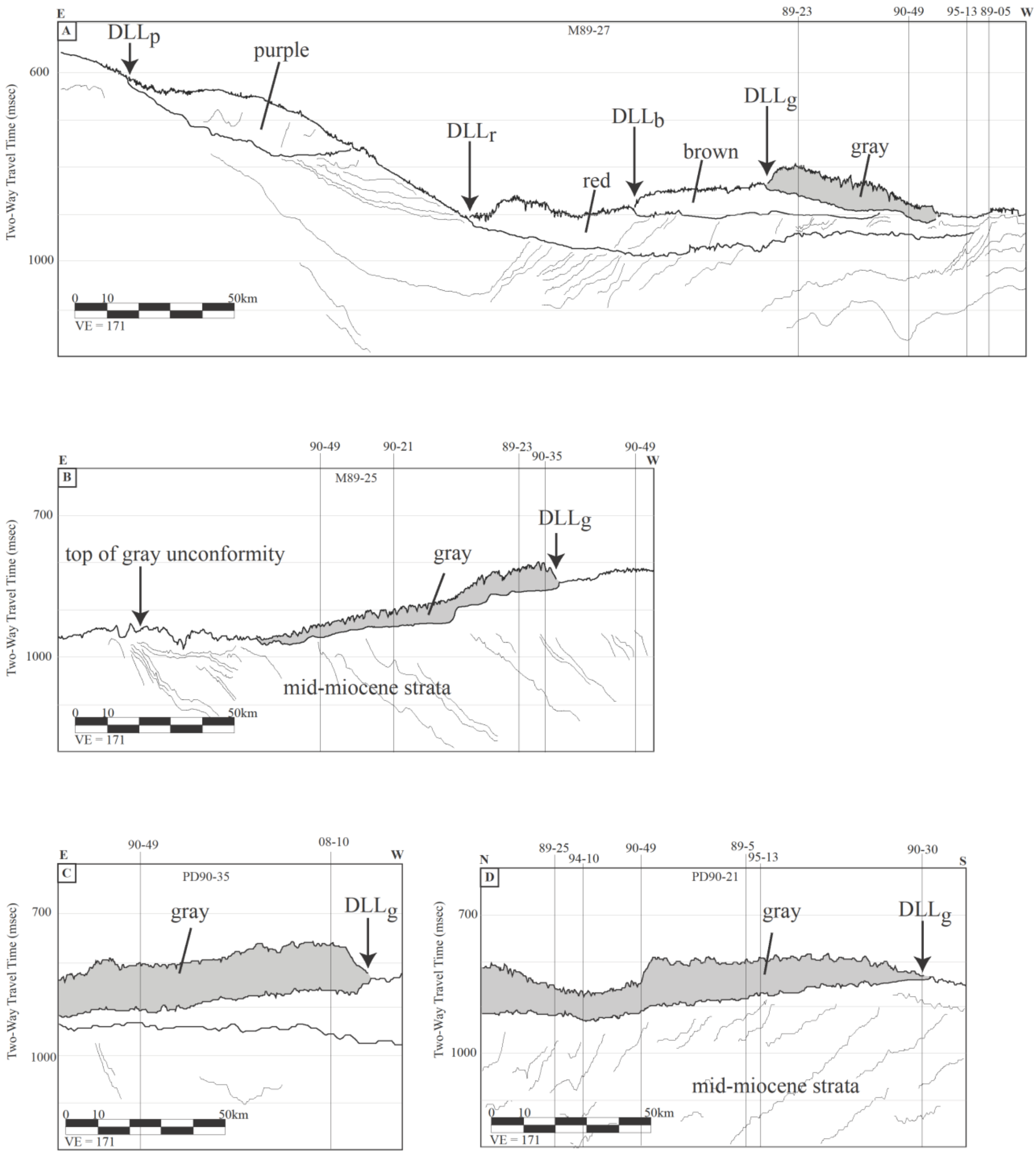

Figure 4. Line drawing interpretations of seismic profiles showing the top and base of the Gray GZW on the middle shelf within Glomar-Challenger-Basin. Seismic line M89-27; Seismic line M89-25; Seismic line PD90-35; Seismic line PD90-21; Seismic line PD90-20; Seismic line NBP94-16; Seismic line NBP0811; Seismic line NBP0810; Seismic line NBP0808; and Seismic line NBP0817. See Figure 5 for the locations of profiles.

(Figure 4 continued)

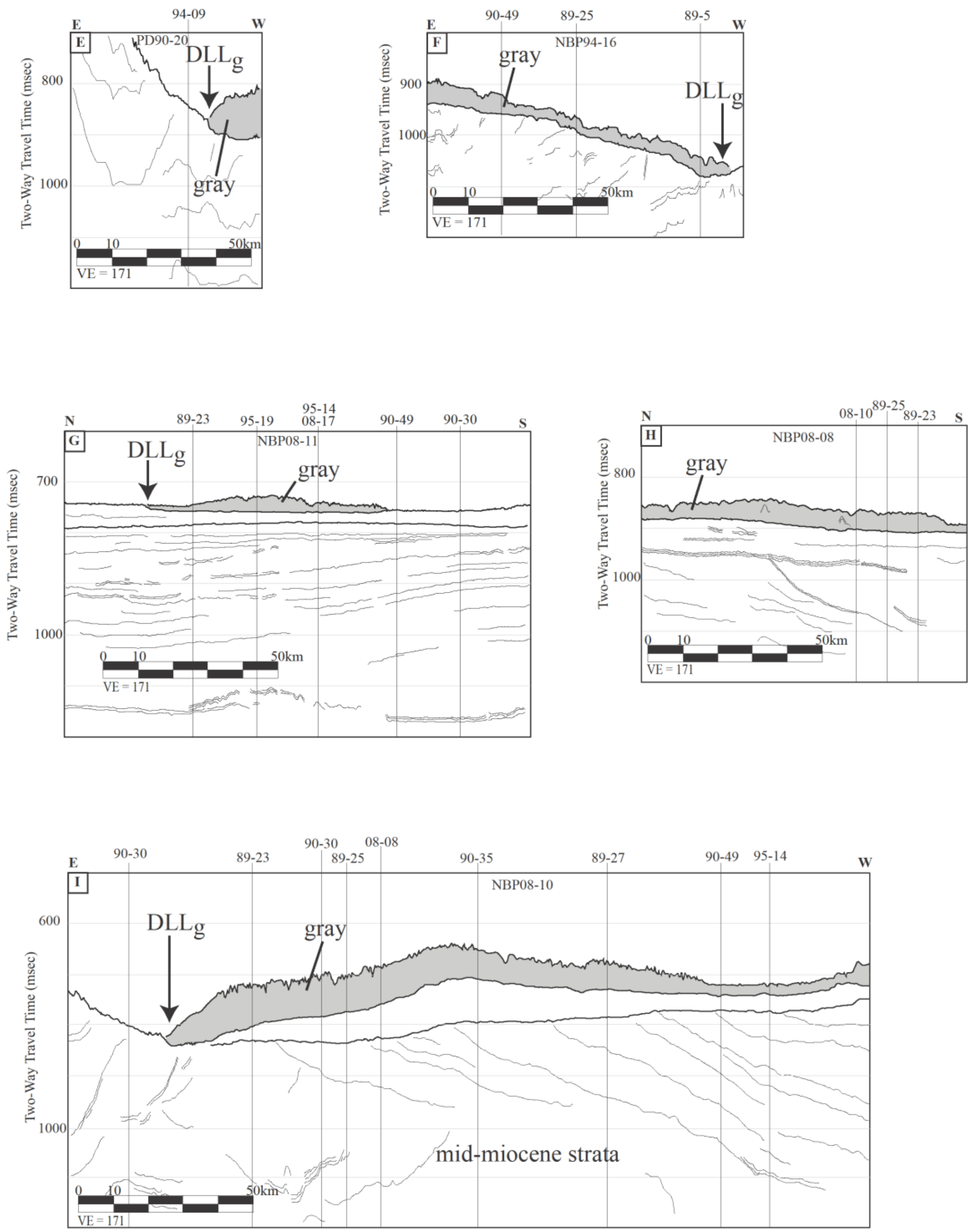

(Figure 4 continued)

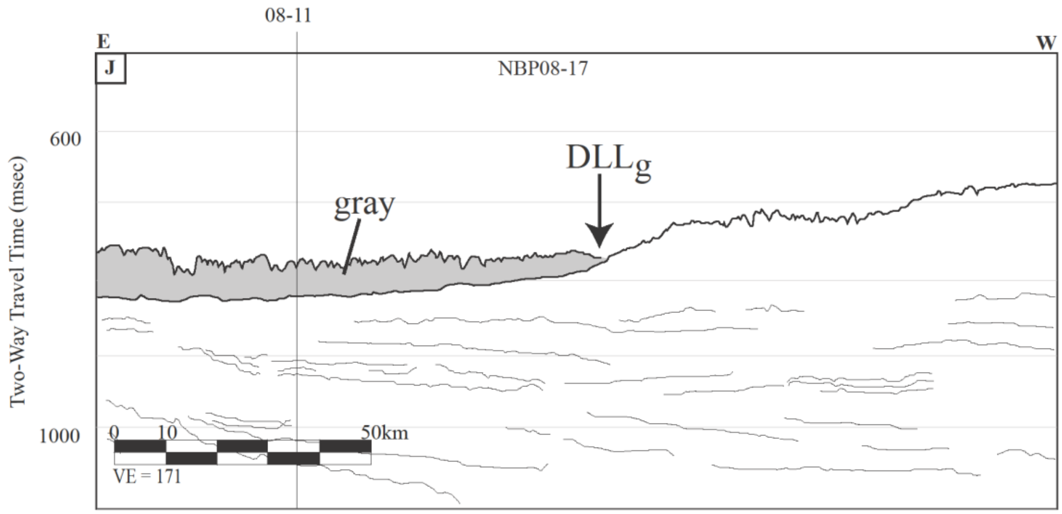

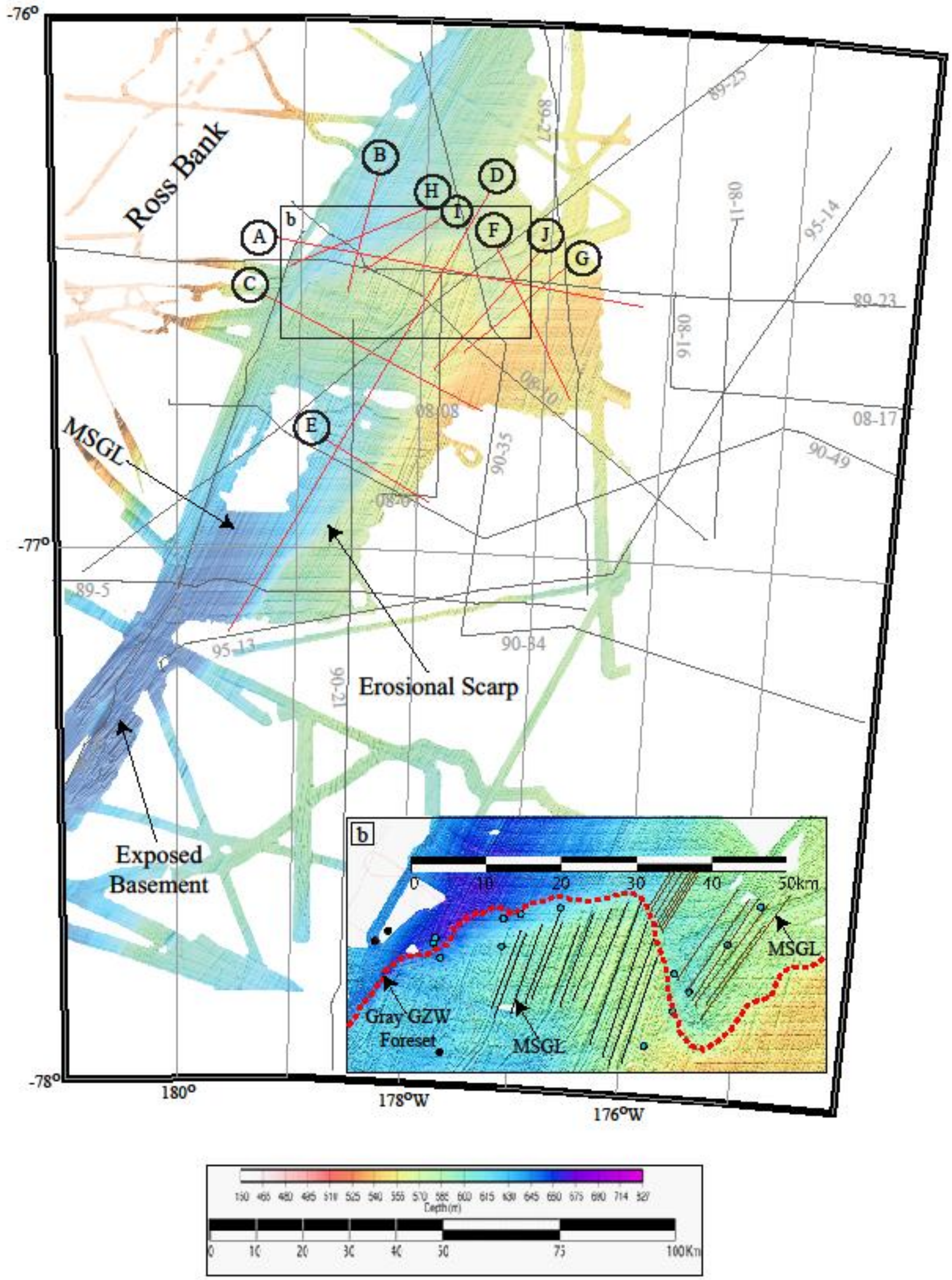

Figure 5. Multibeam survey showing the outline of the Gray GZW interpreted from a synthesis of the seismic and multibeam data. Gray lines show locations of seismic lines, while dashed red lines show the locations of the cross sections from Figure 7A-I.

The large area of the multibeam survey also reveals that some ramps are actually erosional scarps as opposed to foreset dip surfaces (Figures 5 and 6E).

Seismic Stratigraphy and Distribution of the Gray Unit GZW

Correlations of the Gray-Unit GZW on seismic profiles and multibeam data in strike and dip orientations are shown in Figures 4 and 6. These seismic data show the 3D subsurface distribution of Gray GZW thickness (Figure 7). The isopach map also shows that the Gray Unit GZW is confined to the middle shelf by a southward pinchout limit. The unit has few internal reflections but where present, these surfaces dip in a basinward direction (Figure 4A). The correlation of the top and base of the Gray GZW shown on the seismic based line drawings (Figure 4) are based on the 2D correlations of these stratal surfaces as shown on seismic line M89-27 (Figure 3). The top of Gray GZW time-structure contour map (Figure 8) corresponds to the seafloor reflection over much of the map area. This seafloor reflection thus corresponds to the top of the Gray GZW in these regions. The base of the Gray Unit GZW time-structure contour map (Figure 9) corresponds to the top of Brown GZW Unconformity (Figure 4A). In some places, this unconformity corresponds to the top of the Brown GZW, but in other places, the Brown Unconformity also erodes directly into middle Miocene strata (Figures 4B and 4I). The top and base topography of the Gray Unit (Figures 8 and 9) shows that the Gray GZW was deposited in the deep axis of the Glomar Challenger Basin between Ross Bank to the west and a lower elevation bank to the east (Figure 2).

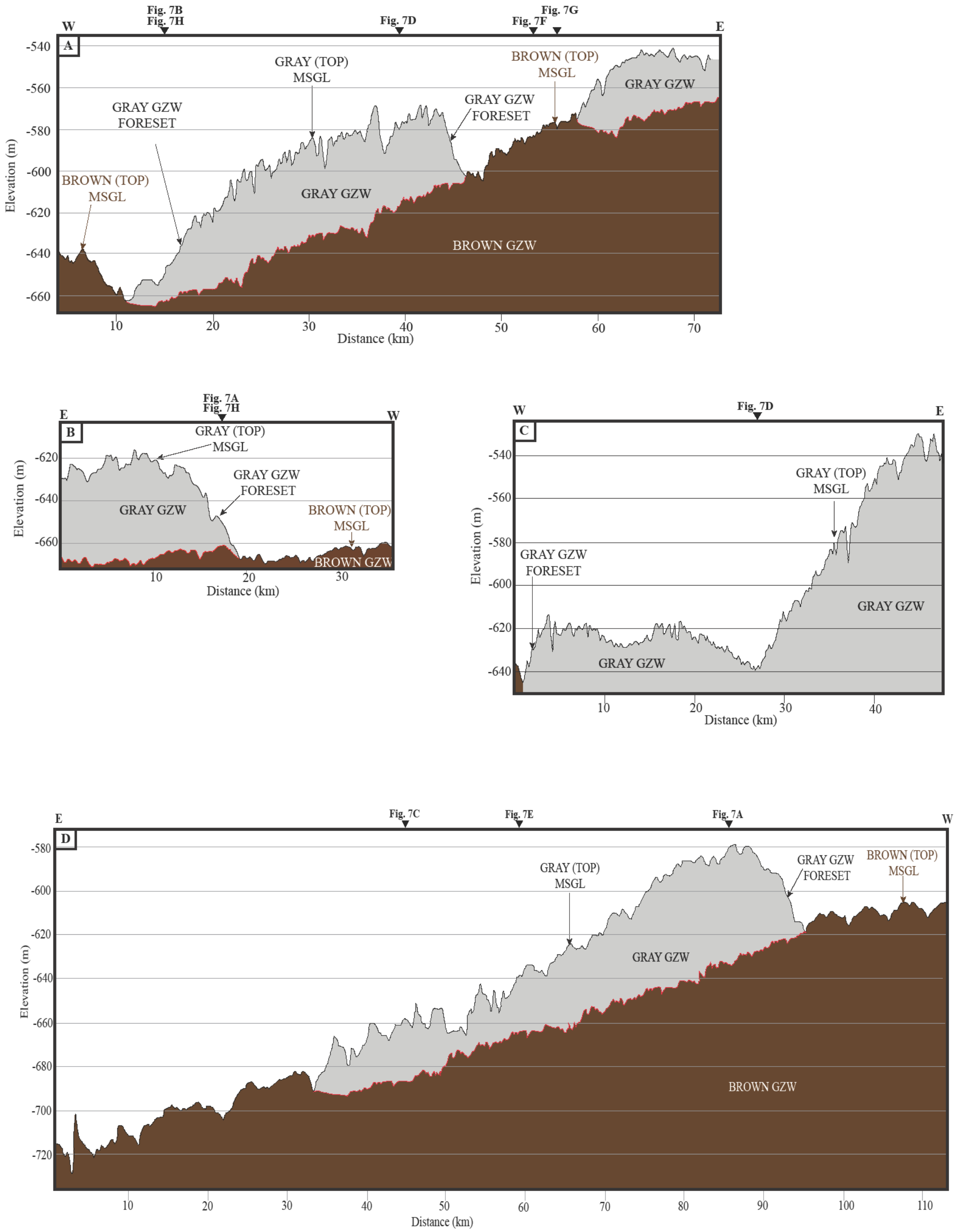

Figure 6: A-J. Interpreted cross sections of the multibeam survey generated in MB systems software showing the topography of the Gray GZW as well as our interpretation of the subsurface stratigraphy based on the regional seismic stratigraphic framework.

(Figure 6 continued)

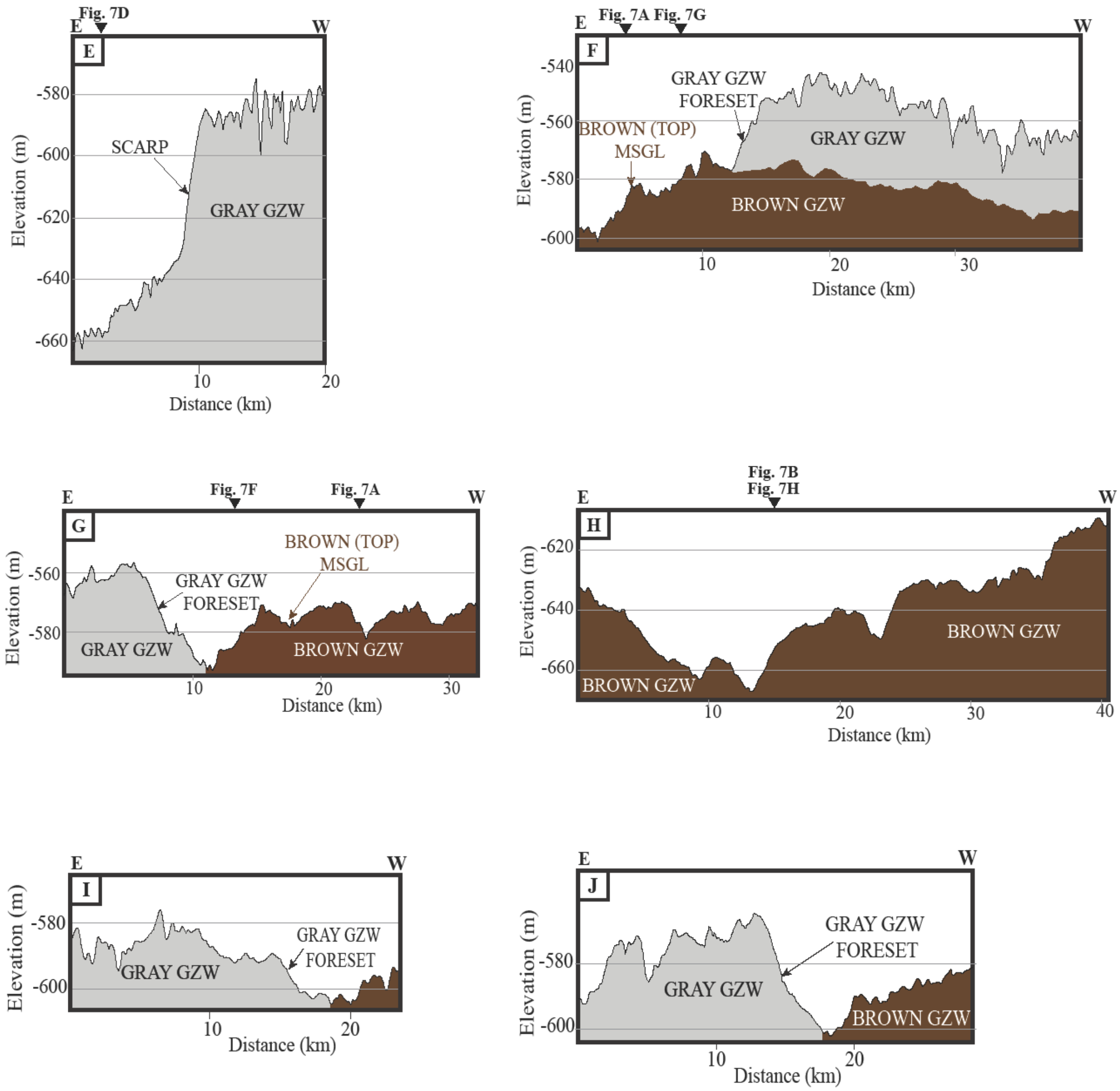

Estimation of the Gray-Unit Grounding-Event Duration Based on a 3D Volume of the Gray Unit GZW

The Gray Unit GZW isopach map (Figure 7) shows that its basinward limits conform to the boundary as shown on the multibeam map (Figure 5). The Gray Unit GZW is at least 140 kilometers wide and occupies most of the Glomar-Challenger-Basin. The maximum and minimum dip-oriented dimension of the GZW ranges from 100 to 20 kilometers. The thickness of the wedge is variable, but averages 30 meters (Figure 7). The volume of the Gray GZW was calculated using a range of velocity estimates (Table 5A-D).

The duration of the Gray GZW deposition was calculated using minimum, intermediate and maximum estimates for the modern and LGM fluxes (see Methods) using the volume from column B in Table 5. For the minimum modern 3D flux, the durations of the Gray Unit grounding event would have taken from 465 kyr (Table 6 column B) based on minimum Whillans Ice Stream width of 30 km. For the maximum modern flux, the duration would have been 69.8 kyr. Using the minimum and maximum LGM fluxes, the durations of the Gray Unit grounding event would have taken from 116.4 kyr to 17.5 kyr (Table 6 column C). All of these durations are far longer than the duration of the short post-LGM timeframe.

Table 5. 3D volume estimates of the gray GZW using different sediment velocity estimates

	Volume			
	A 1500 m/s	**B** 1750 m/s	**C** 2000 m/s	**D** 2250 m/s
Gray	2.39×10^{12} m^3	2.79×10^{12} m^3	3.19×10^{12} m^3	3.58×10^{12} m^3

.

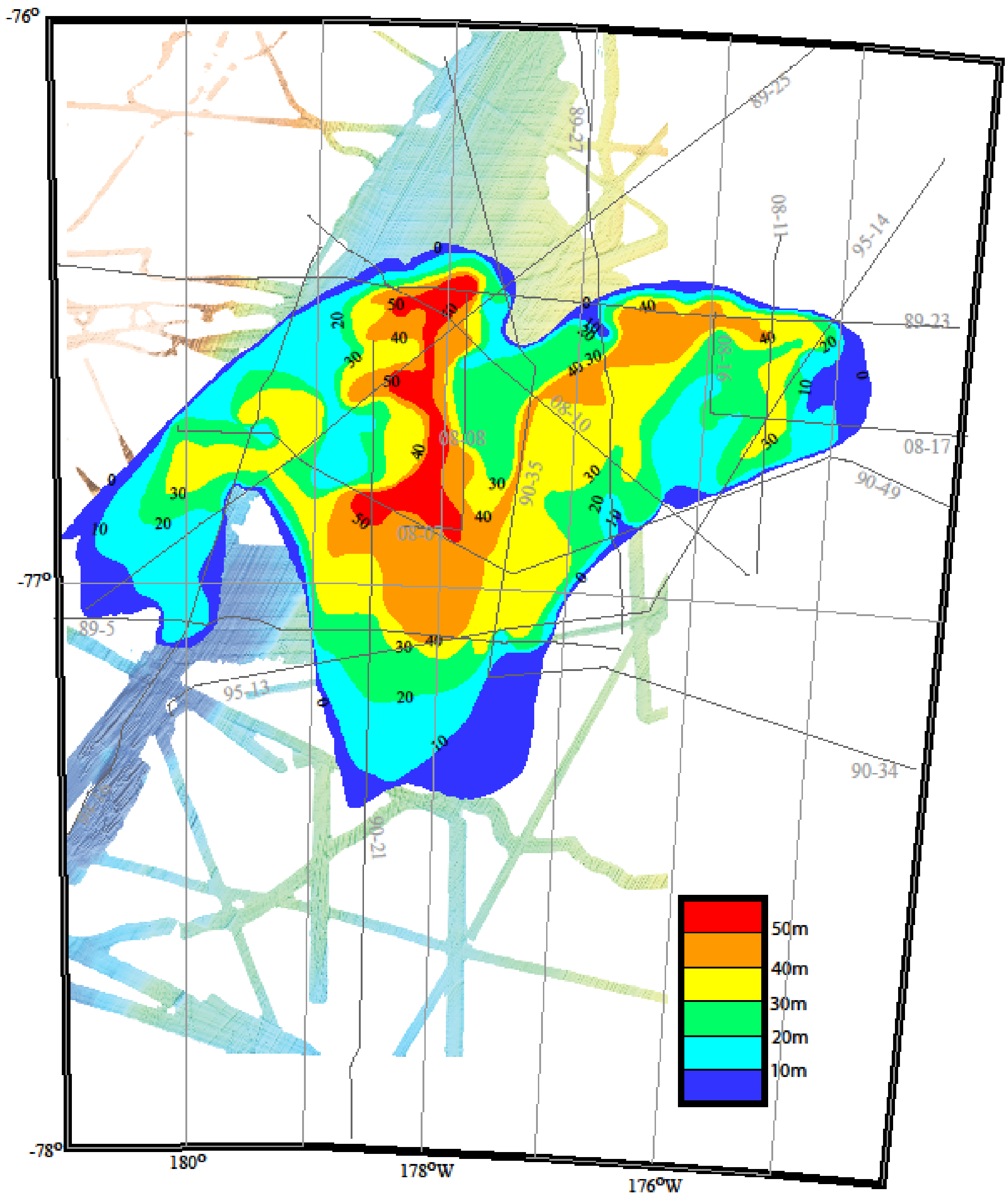

Figure 7. Color coded isopach map of the Gray Unit GZW generated from the seismic interpretations presented in Figure 4. The basinward edge of the GZW corresponds to a depositional pinchout. The landward edge corresponds to an erosional truncation limit associated with subglacial erosion of the WAIS. The contour interval is 10 meters.

Figure 8. Time-structure contour map at the top of the Gray Unit GZW. The map was constructed using the seismic interpretations shown in Figure 4. The thick black line shows the outline of the Gray Unit GZW. The contour interval is 50 milliseconds two-way travel time, which is equivalent to ~44 m using a sediment velocity of 1750 m/s.

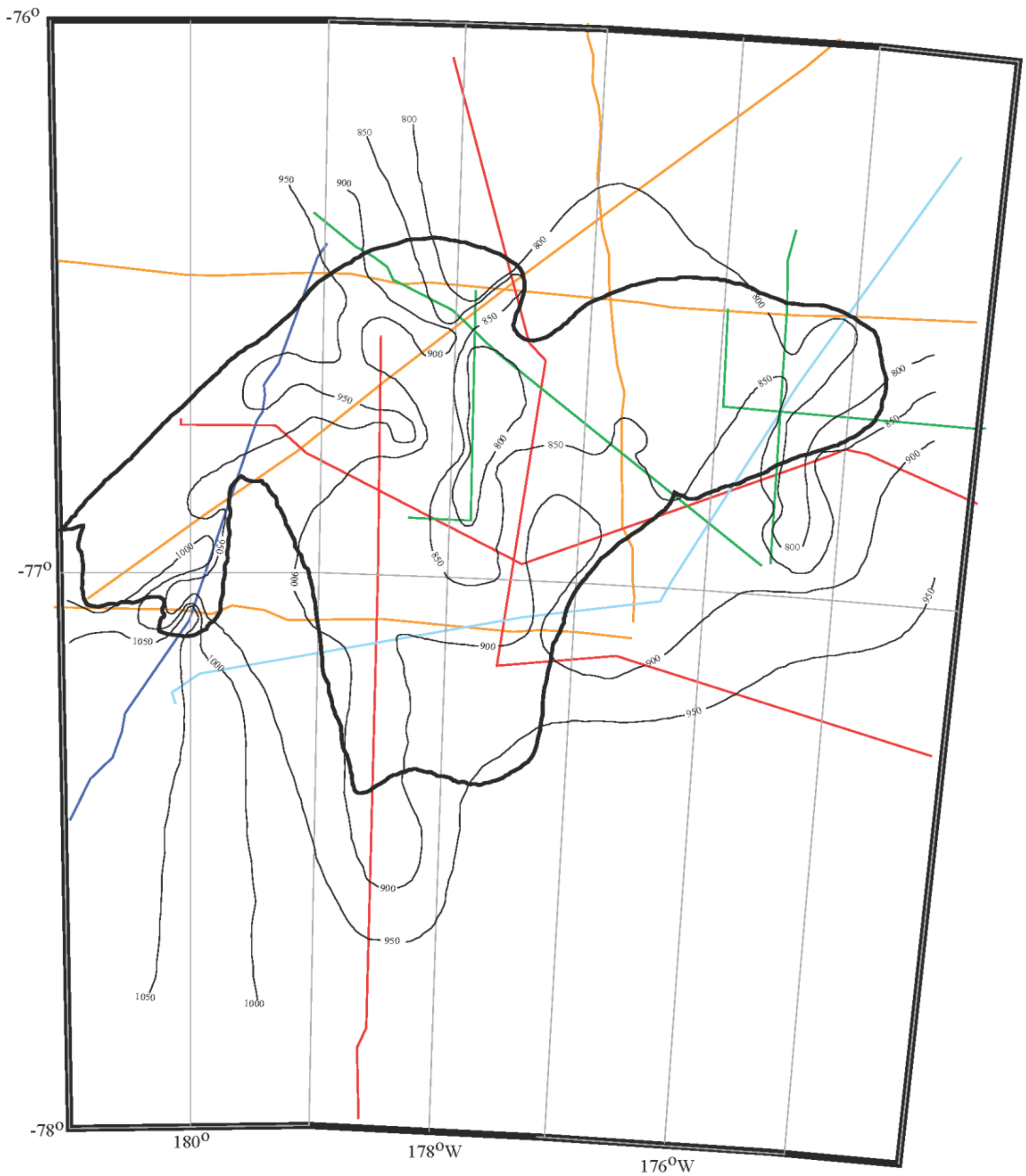

Figure 9. Time-structure contour map at the base of the Gray Unit GZW. The map was constructed using the seismic interpretations shown in Figure 4. The thick black line shows the outline of the Gray Unit GZW. The contour interval is 50 milliseconds two-way travel time, which is equivalent to ~44 m using a sediment velocity of 1750 m/s.

Table 6. Gray grounding event durations assuming sediment velocity of 1750 m/s, using 3D modern flux, 3D LGM flux, and a temperate flux computed from Dowdeswell et al. (2010). Associated yields for East Antarctica and West Antarctica for the Glomar-Challenger-Basin at LGM, and the temperate system from Dowdeswell et al. (2010).

GZW	**A** GZW Volume (m^3)	**B** Durations using 3D Modern flux			**C** Durations using 3D LGM flux			**D** Durations using Temperate Flux
		Min (30km)	Int (100 km)	Max (200 km)	Min (30km)	Int (100 km)	Max (200 km)	
		$6x10^6$ m^3/a	$2x10^7$ m^3/a	$4x10^7$ m^3/a	$2.4x10^7$ m^3/a	$8.0x10^7$ m^3/a	$1.6x10^8$ m^3/a	2.8×10^8 m^3/a
Gray	2.79×10^{12}	465 kyr	139.5 kyr	69.8 kyr	116.4 kyr	34.9 kyr	17.5 kyr	9.4 kyr

YIELDS						
	East Antarctica $m^3/m^2/a$			West Antarctica $m^3/m^2/a$		
	Min (30km)	Int (100km)	Max (200 km)	Min (30km)	Int (100km)	Max (200 km)
Glomar-Challenger-Basin at LGM	1.785×10^{-5}	5.95×10^{-5}	1.19×10^{-4}	2.55×10^{-5}	8.5×10^{-5}	1.7×10^{-4}
Temperate Yield from Dowdeswell et al. (2010)	2.4×10^{-4}			3.12×10^{-4}		

Discussion

Evaluation of the 2D Based Estimates of Grounding Event Durations

In all cases, the grounding-event durations estimated using the 2D approach suggest that the three GZWs within the Glomar Challenger Basin contain too much volume to have been deposited during a short post-LGM timeframe if either the modern or LGM flux were active (Table 4 columns B and C, respectively). The use of the 1750 m/s velocity for Time-Depth conversion (Table 3 Column B) is supported by velocity analysis in Eastern Ross Sea continental shelf which reports similar velocity values for the shallow subsurface levels (Cochrane et al., 1995). Nonetheless, the calculated durations do not vary by a significant amount even if end-member velocity values are used to make the time-depth conversion. We focus on the durations calculated from maximum LGM flux because flux is expected to be higher when the drainage basin was larger. On the basis of the maximum LGM 2D flux, the 11.5 kyr total durations of the three grounding events is ~3.5 times longer than the 3200 year post-LGM timeframe (Table 4). This long-durations tend to suggest that the three units (the Red, Brown and Gray GZWs) could not have been deposited during the brief post-LGM timeframe.

For the three GZWs to have been deposited during the 3200 year post-LGM timeframe, the flux would have had to have been an order of magnitude higher than the inferred maximum LGM 2D flux (Table 4 column D). We reject this possibility because this higher minimum required flux would require that West Antarctic yields for the LGM drainage basin would have had to significantly exceeded the modern yield by 20.5 times using maximum estimate for modern GZW width (e.g. 1.7×10^{-4} $m^3/m^2/a$ vs. 3.48×10^{-3}

$m^3/m^2/a$, Table 6). The yield for the higher minimum required flux of 4102.2 $m^3/m^2/a$ was calculated by extrapolating the 2D flux to 3D by multiplying it by the maximum estimate of the Whillans Ice Stream width (200 km). The result is the divided by the Whillans drainage area. Although the flux may have been higher by virtue of the larger drainage area at LGM, the yield is unlikely to have been higher than that existing in the modern. Moreover, if the three GZWs were associated with the post-LGM retreat, then the Glomar-Challenger-Basin paleotrough probably would have already been scoured of the most easily sediments that were deposited during the advance of grounded ice to the outer shelf.

While these 2D results seem to preclude the possibility that the three GZWs could have been deposited during the post-LGM timeframe, they clearly do not strongly support the alternate view advanced by Bart and Cone (2011). In other words, the durations are far shorter than anticipated if it were that each of the three GZWs actually represented deposition during three discrete 100 kyr glacial cycles. In other words, the 3 GZWs contain too little volume to have been deposited during long durations spanning all or part of the last glacial cycle.

Data generated in the 2D (and 3D) experiments revealed two potential problems of using a 2D approach. The first potential source of error concerns the assumption that the modern flux for the Whillans Ice Stream GZW is accurately calculated. The Anandakrishnan et al. (2007) estimate relied on a single cross section of the Whillans GZW. The actual orientation of the cross section is at approximately 30° to the direction of ice-stream flow and thus it is not a true dip-oriented transect. Given that the section is not a true dip line, the slice volume measured may not be good dip-oriented representation of the average slice volume of the modern Whillans GZW. Moreover, the Whillans GZW width is not known. If the Whillans GZW is not extensive, i.e., 30 km wide, the calculated time to deposit the 3 GZWs would be 77 kyr, i.e., ~7 times longer than inferred if the GZW is 200 km wide. Given the uncertainty of the modern GZW extent, the estimate of 2D flux should be used with caution until more data are available to confirm this flux estimate. One possibility is that the cross section volume measured for the modern ice stream GZW may thus represent an over-estimation of the modern flux. Indeed, if the modern flux is overestimated, then the durations we calculated for the three GZWs in the Glomar Challenger Basin may be shorter than actual.

A second source of error associated with the 2D approach concerns how well M89-27 measures the 2D slice volume of the three GZWs. It is observed that the cross-section slice volumes of the Gray Unit GZW show significant variability (Table 7). These cross-section slice volumes demonstrate that the 3D thickness distribution of the Gray Unit GZW is sufficiently variable that no 2D line generates what qualifies as the average 2D cross-section slice volume from which a grounding event duration might be demonstrable more correct than a calculation based on another 2D cross-section slice volume. The largest cross-section volume comes from seismic line 08-10 (Table 7) which obliquely crosses the GZW with respect to the dip orientation of ice-stream flow as indicated by the orientation of MSGLs. The volumes of the three GZWs on seismic line M89-27 (Figure 3) are smaller than the average cross-section volume, then the durations calculated are too short. For example, using the maximum cross-section sediment volume on NBP08-10 (Figure 4I), the duration of the Gray GZW would be 6.4 kyr whereas using the minimum cross-section volume, the duration would be 0.6 kyr (Table

7). The average cross-section slice from the 3D volume would give a duration of 17.5 kyr (i.e., the duration deduced from the 3D analysis). Since the Gray GZW is demonstrably not a line source feature, the results from the 2D experiment should be considered invalid because the durations calculated significantly depend on the cross section used.

Table 7. Grounding event durations of the Gray GZW from different seismic profiles assuming sediment velocity of 1750 m/s, using 2D modern flux of 200 m^3/m/yr, 2D LGM flux based on minimum estimate of Whillans Ice Stream Width (30 km) of 853.3 m^3/m/yr, and a minimum required flux (4102.2 m^3/m/yr).

Seismic Line	Gray GZW Volume (m^3)	Estimated Durations (kyr)		
		2D modern flux (200 m^3/m/yr)	2D LGM flux (1141.8 m^3/m/yr)	Minimum required flux (4102.2 m^3/m/yr)
90-20	5.38×10^5	2.69	0.5	0.1
08-11	1.42×10^6	7.1	1.24	0.3
94-16	1.44×10^6	7.2	1.26	0.4
08-08	1.67×10^6	8.35	1.46	0.4
89-25	1.89×10^6	9.45	1.66	0.5
89-27	2.30×10^6	11.5	2.01	0.56
90-21	5.02×10^6	25.1	4.4	1.22
90-35	5.06×10^6	25.3	4.4	1.23
08-10	5.53×10^6	27.7	4.8	1.35

Evaluation of the 3D Based Estimates of Grounding Event Durations

The durations needed to deposit the 3D volume measurement for the Gray GZW far exceed the duration of the post-LGM time frame for both the modern 3D fluxes and the LGM 3D fluxes (Table 6). All calculated durations preclude the post-LGM interpretation of the GZWs. The 116.4 kyr duration estimate (Table 6) based on the inferred LGM 3D flux for the minimum Whillans Ice Stream width is about 120% of the 100 kyr period of the last glacial cycle. This minimum Whillans Ice Stream width calculations tend to support the view that the Gray GZW represents the amalgamation of erosion and deposition during the majority of the last glacial cycle. However, it is unlikely that the flux was this low (i.e., that the modern GZW is only 30 km wide) and hence we reject the view that the Gray GZW represents a depositional episode spanning all of the last glacial cycle from OIS 5 to OIS 2.

Table 8. 2D and 3D LGM flux rate generated for minimum, intermediate and max ice stream width for the Whillans Ice Stream.

Flux Type	Min (30km)	Intermediate (100km)	Max (200 km)
2D LGM Flux	171.207 $m^3/m/a$	570.67 $m^3/m/a$	1141.837 $m^3/m/a$
3D LGM Flux	2.397×10^7 m^3/a	7.989×10^7 m^3/a	1.599×10^8 m^3/a

At the other extreme, the maximum flux (calculated for the maximum 200 km width estimate of the Whillans Ice Stream) gives a 17.5 kyr duration with represents ~20% of the last glacial cycle. In this scenario, the Gray GZW may represent deposition beginning in OIS 3 at approximately 42 ka ^{14}C BP and culminating at 25 ^{14}C ka BP as the WAIS reached the middle shelf (Figure 10). If this view is correct, the Brown GZW may represent deposition during the first part of the last glacial cycle (i.e., from OIS 5d – OIS 4). The large volume of the Red GZW may then represent deposition during the entirety of the previous glacial cycle, i.e., from OIS 7 to OIS 6. The 17.5 kyr duration represents the shortest (most conservative) possible time for the Gray GZW grounding event because the calculation relies on a maximum possible flux. Moreover, the calculations applied the modern yield to the larger LGM drainage basin. However, data from Elverhoi et al. (1998) suggest that yield decreases as drainage area increases. In other words, it is possible that the grounding event took longer, but it is not likely that the grounding event was shorter than 17.5 kyr.

Conceptual Model of Middle Shelf GZW Construction during the 100 kyr Advance Phase of the Last Glacial Cycle

Figure 10 shows the interpretations of how the Gray GZW was constructed. The last glacial cycle was arbitrarily subdivided into 5 equal 20 kyr intervals of sedimentation. Stage 1 (Figure 10A) represents OIS 5e. At OIS 5e, the WAIS stabilized in a position close to the modern grounding line. Flux at OIS 5e would have been similar to that currently existing at Whillans Ice Stream (Table 6; maximum flux in column B). As the WAIS advanced, the size of the drainage basin increased progressively and thus the flux would have increased as the extent of grounded ice expanded northward. The flux continually supplied sediment at an increasingly higher rate from OIS 5e (Stage 1, Figure 10A) to a maximum flux at OIS 2 (Stage 6, Figure 10F) equivalent to the inferred maximum 3D LGM flux used in the calculations shown in Table 6 (column C). It is inferred that the preservation potential of the newly constructed GZW was negligible during the advance phase of last glacial cycle. This inference is consistent with seismic based observations showing that the dip-oriented extent of the Gray GZW is limited. Thus, volume of the GZW is successively larger during each 20 kyr interval and includes the new sediment flux plus the sediment flux from short-distance recycling of the GZW deposited during the preceding 20 kyr interval. This flux thus built the Brown GZW from OIS 5e (Stage 1) till OIS 4 (Figure 10E). In this scenario, the WAIS retreated at OIS 3 to end the Brown Unit grounding event. The Gray GZW was deposited from OIS 3 to OIS 2 (Stage 6, Figure 10F). The duration between OIS 3 and OIS 2 is close to the 23.3 kyr duration calculated for the Gray GZW. Based on this model (Figure 10), the predicted 3D volume of the Brown GZW is 6×10^{12} m^3 at the culmination of stage 4. At OIS 3, the WAIS began to deposit the Gray Unit GZW.

If the line of reasoning in this study is accepted, the Gray GZW is assigned to deposition from OIS 3 to OIS 2, whereas the Brown GZW is assigned to deposition occurring during the first part of the last glacial cycle from OIS 5e – OIS 4. Given the large volume of the Red GZW, this unit may represent the amalgamation of the last 100 kyr glacial cycle (OIS 7 – OIS 6).

Figure 10. Six-stage conceptual model showing the advance of grounded ice from an inner shelf to a middle shelf position over a 100 kyr period of the last glacial cycle. A) Grounded ice stabilized at the OIS5e peak of the last interglacial at 125 kyr BP. The grounding line position is taken to be equivalent to the modern interglacial position. B) Expanded position of the grounding line at 105 kyr BP showing the accumulation of GZW that advances by progradation at its seaward termination and erosion at its landward end. C) At 85 kyr BP, showing the advance position of the GZW and the larger volume corresponding to the larger flux plus short-distance recycling of the wedge deposited in stage B. D) Position and volume of the Gray GZW at 65 kyr BP. E) Position and volume of the Gray GZW at 45 kyr. F) Position and volume of the Gray GZW at 25 kyr on the middle shelf. G) Stable position of the grounded ice 1000 years prior to the present before the onset of modern GZW deposition at Whillans Ice Stream.

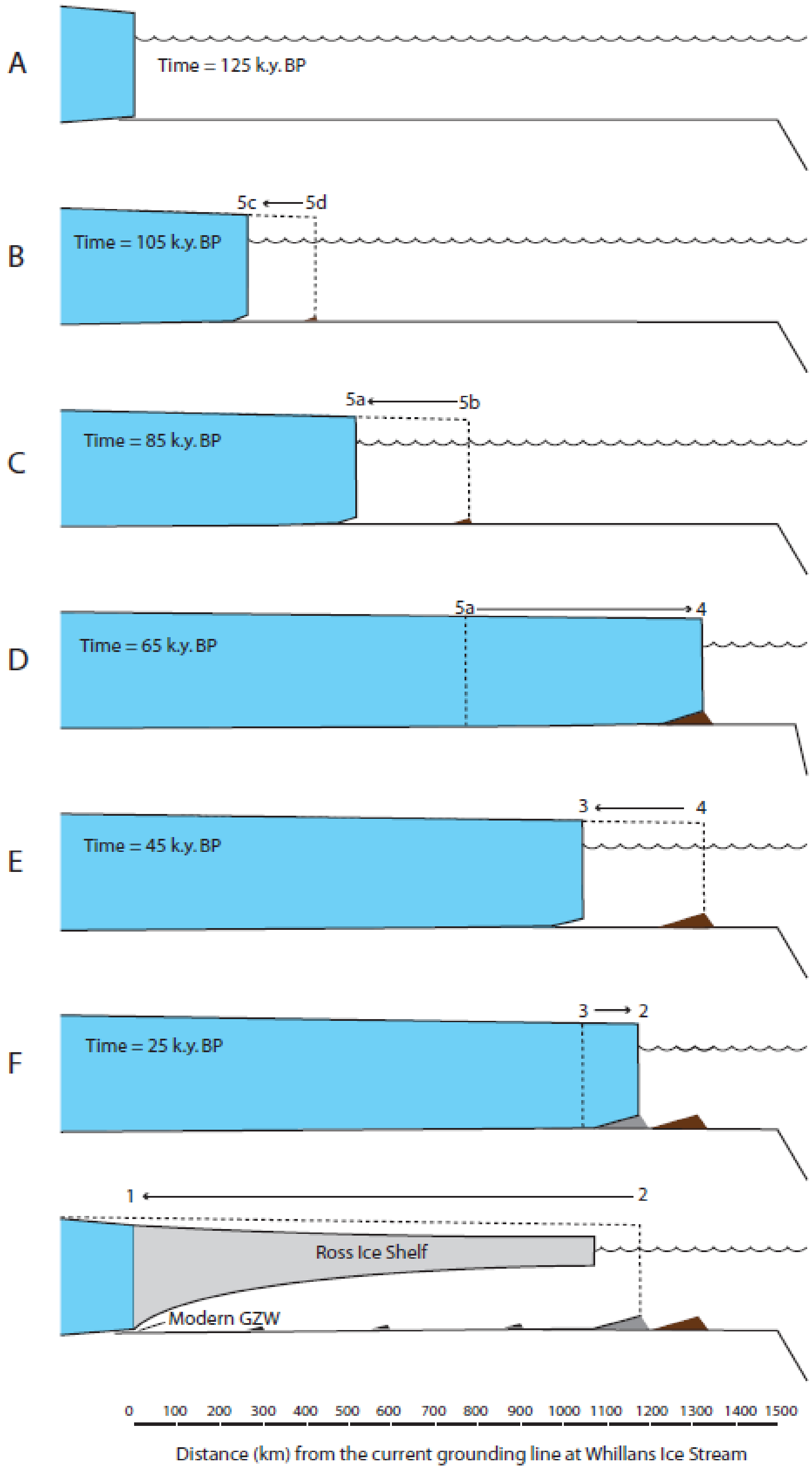
A
Time = 125 k.y. BP
B
5c
5d
Time = 105 k.y. BP
C
5a
5b
Time = 85 k.y. BP
D
5a
4
Time = 65 k.y. BP
E
3
4
Time = 45 k.y. BP
F
3
2
Time = 25 k.y. BP
1
2
Ross Ice Shelf
Modern GZW
0 100 200 300 400 500 600 700 800 900 1000 1100 1200 1300 1400 1500
Distance (km) from the current grounding line at Whillans Ice Stream

Conclusions

All durations calculated using the 2D approach (i.e., line M89-27) suggests that the GZWs in the Glomar Challenger Basin contain too much volume to have been deposited in 3200 years. However, the results of the 2D experiment are considered suspect because the Gray GZW clearly is not a line source. In other words, the estimated duration depends on the cross section evaluated. The accuracy of the durations using the 3D approach is dependent on the validity of the 2D flux reported by Anandakrishnan et al. (2007). The 3D calculations demonstrate that the Gray GZW in the Glomar Challenger Basin was deposited over a time interval at least one order of magnitude longer than the post-LGM timeframe permits. Furthermore, for the Gray GZW unit to have been deposited in a post-LGM timeframe, the flux would have to have been an order of magnitude higher (2.6×10^9 m^3/a) than the maximum estimate of flux used in this study. The relatively long duration needed to deposit the GZW (17.5 kyr) favors the view that the Gray Unit was deposited during WAIS advance from OIS 3 to OIS 2. If this interpretation is correct, the Brown GZW may have been deposited from OIS 5e to OIS 4. In this scenario, the Red GZW would be attributed to the previous glacial cycle (OIS 7 – OIS 6).

References

Anandakrishnan, S. Catania, G.A., Alley, R.B., Horgan, H.J., 2007. Discovery of Till Deposition at the Grounding Line of Whillans Ice Stream. *Science*, 315, 1835-1838.

Anderson, J. B., Andrews J. T., 1999. Radiocarbon constraints on ice sheet advance and retreat in the Weddell Sea, Antarctica. *Geology*, 27, 179-182

Anderson, J. B., Shipp, S. S., Lowe, A. L., Wellner, J. S., Mosola, A. B, 2001. The Antarctic Ice Sheet during the Last Glacial Maximum and its subsequent retreat history: a review. *Quaternary Science Reviews*, 21, 49-70.

Anderson, J., 2007. Ice sheet stability and sea-level rise. *Science*, 315, 1803-1804.

Shipp, S., Anderson, J., and Domack, E., 1999, Late Pleistocene-Holocene retreat of the West Antarctic Ice-Sheet system in the Ross Sea: Part 1 – Geophysical results. *GSA Bulletin*, 111, 1486-1516.

Bamber, J., 2009. Reassessment of the potential sea-level rise from a collapse of the West Antarctic ice sheet. *Science*, 324, 901-903.

Bart, P.J., 2004, West-directed flow of the West Antarctic Ice Sheet across Eastern Basin, Ross Sea during the Quaternary. *Earth and Planetary Science Letters*, 228, 425-438.

Bart, P. J., Cone, A. N., 2011. Early stall of West Antarctic Ice Sheet advance on the eastern Ross Sea middle shelf followed by retreat at 27,500 ^{14}C yr BP. *Palaeogeography, Palaeoclimatology, Palaeoecology*, Available online 3 September 2011, (http://www.sciencedirect.com/science/article/pii/S0031018211004330)

Bentley, C. R., and Jezek, K. C., 1981. RISS, RISP, and Riggs: Post-IGY glaciological investigation of the Ross Ice Shelf in the U.S. program. *Journal of the Royal Society of New Zealand*, 11, 355-372.

Bohm, G., Ocakoglu, N., Picotti, S., De Santis, L., 2009. West Antarctic Ice Sheet evolution: New insights from a seismic tomographic 3D depth model in the Eastern Ross Sea (Antarctica). *Marine Geology*, 266, 109-128.

Chow, J. M., Bart, P. J., 2003. West Antarctic Ice Sheet grounding events on the Ross Sea outer continental shelf during the middle Miocene. *Palaeogeography, Palaeoclimatology, Palaeoecology*, 198, 169-186.

Clough, J. W., Hansen, B. L., 1979. The Ross Ice Shelf Project. *Science*, 203, 433-434.

Cochrane, G. R., De Santis, L., and Cooper, A. K., 1995. Seismic velocity expression of glacial sedimentary rocks beneath the Ross Sea from sonobuoy seismic-refraction data, *Antarctic Research Series*, 68, in: A.K. Cooper, P.F. Barker, G. Brancolini, Editors , *Geology and seismic stratigraphy of the Antarctic Margin*, 261–270.

Conway, H., Hall, B.L., Denton, G.H., Gades, A.M., and Waddington, E.D., 1999, Past and future grounding-line retreat of the West Antarctic Ice Sheet. *Science*, 286, 280-283.

Conway, H., Catania, G., Raymond, C. F., Gades, A. M., Scambos, T. A., Engelhardt, H., 2002. Switch of flow direction in an Antarctic ice stream. *Nature*, 419, 465-467.

Cowan, E. A., Seramur, K. C., Powell, R. D., Willems, B. A., Gulick, S. P. S., Jaeger, J. M., 2010. Fjords as temporary sediment traps: History of glacial erosion and deposition in muir inlet, glacial bay national park, southeastern Alaska. *Geological Society of America Bulletin*, 122, 1067-1080.

Domack, E.W., Jacobsen, E.A., Shipp, S., Anderson, J.B., 1999, Late Pleistocene-Holocene retreat of the West Antarctic Ice Sheet system in the Ross Sea: Part 2 – Sedimentologic and stratigraphic signature. *GSA Bulletin*, 111, 1517-1536.

Dowdeswell, J. A., Ottesen, D., Evans, J., Cofaigh, C. O., Anderson, J. B., 2008, Subglacial landforms and rates of ice-stream collapse. *Geology*, 38, 819-822.

Dowdeswell, J. A., Ottesen, D., Rise, L., 2010. Rates of sediment delivery from the Fennoscandian Ice Sheet through an ice age. *Geology*, 38, 3-6.

Graham, A. G., Larter, R. D., Gohl, K., Dowdeswell, J. A., Hillenbrand, C., Smith, J. A., Evans, J., Kuhn, G., Deen, T., 2010. Flow and retreat of the Later Quaternary Pine Island-Thwaites palaeo-ice stream, West Antarctica. Journal of Geophysical Research, 115, F03025.

Hallet, B., Hunter, L., Bogen, J., 1996. Rate of erosion and sediment evacuation by glaciers: A review of field data and their implications. *Global and Planetary Change*, 12, 213-235.

[1]Heinrich, P, 2005. Colored Shaded Relief Map of Subglacial Topography and Bathymetry of Antarctica <http://members.cox.net/pyrophyllite/bedrock.html>

Koppes, M., Hallet, B., 2006. Erosion rates during rapid deglaciation in icy bay Alaska. *Journal of Geophysical Research*, 111, F02023.

Laberg, J. S., Eilersten, R. S., Vorren, T. O., 2009. The paleo-ice stream in Vestfjorden, north Norway, over the last 35 kyr Glacial erosion and sediment yield. Geological Society of America Bulletin, 121, 434-447.

Licht, K.J., and Andrews, J.T., 2002, The ^{14}C record of late Pleistocene ice advance and retreat in the central Ross Sea, Antarctica. *Arctic, Antarctic, and Alpine Research*, 34, 324-333.

Lisiecki, L. E., Raymo, M. E., 2005. A Pliocene-pleistocene stack of 57 globally distributed benthic $\delta^{18}O$ records. *Paleoceanography*, 20, PA1003.

Lythe, M. B., Vaughan, D. G. and the BEDMAP Consortium, 2000. BEDMAP - bed topography of the Antarctic. 1:10,000,000 scale map. BAS (Misc) 9. Cambridge, British Antarctic Survey.

Mosola, A.B., and Anderson, J.B., 2006, Expansion and rapid retreat of the West Antarctic Ice Sheet in eastern Ross Sea: possible consequence of over-extended ice streams? *Quaternary Science Reviews*, 25, 2177-2196.

Nygard, A., Sejrup, H. P., Haflidason, H., Lekens, W. A. H., Clark C. D., Bigg, G. R., 2007. Extreme sediment and ice discharge from marine based ice streams: New evidence from the North Sea. *Geology,* 35, 395-398.

Ottesen, D., Rise, L., Knies, J., Olsen, L., Henriksen, S., 2005. The Vestfjorden-Traenadjupet palaeo-ice stream drainage system, mid-Norwegian continental shelf. *Marine Geology*, 218, 175-189.

Parizek, B. R., Alley, R. B., 2003. Ice thickness and isostatic imbalances in the Ross Embayment, West Antarctica: model results. *Global and Planetary Change*, 2004, 265-278.

Peltier, W.R. and R.G. Fairbanks, 2006. Global glacial ice volume and Last Glacial Maximum duration from an extended Barbados sea level record. *Quaternary Science Reviews*, 25, 3322-3337.

Petit, J.R., et al., 2001. Vostok Ice Core Data for 420,000 Years, IGBP PAGES/World Data Center for Paleoclimatology Data Contribution Series #2001-076. NOAA/NGDC Paleoclimatology Program, Boulder CO, USA.

Raymo, M. E., 1997. The timing of major climate terminations. *Paleoceanography*, 12, 577-585.

Rignot, E., Mouginot, J., Scheuchl, B., 2011. Ice Flow of the Antarctic Ice Sheet. *Science*, 333, 1427-1430.

Rignot, E., Thomas, R., 2002. Mass Balance of Polar Ice Sheets. *Science*, 297, 1502-1506.

Schlunegger, F., Melzer, J., Tucker, G., 2001. Climate, exposed source rock lithologies, crustal uplift and surface erosion - a theoretical analysis calibrated with data from the Alps/North Alpine Foreland Basin system. *International Journal of Earth Sciences*, 90, 484-499.

Shipp, S., Anderson, J., and Domack, E., 1999, Late Pleistocene-Holocene retreat of the West Antarctic Ice-Sheet system in the Ross Sea: Part 1 – Geophysical results: *GSA Bulletin*, 111, 1486-1516.

Siegert, M. J., 1999, Antarctic subglacial lakes. *Earth-Science Reviews*, 50, 29-50.

Stockwell, J. W., Cohen, J. K., 2008. The new SU user's manual. Center for wave phenomena, Colorado school of mines. <ftp://ftp.cwp.mines.edu/pub/cwpcodes/sumanual_300dpi_a4.pdf>

Truffer, M., and Echelmeyer, K.A., 2003, Of isbræ and ice streams. *Annals of Glaciology*, 36, 66-72.

Tulaczyk, S., Joughin, I., 2003. Antarctic ice stream dynamics. *AccessScience, ©McGraw-Hill Companies*. <http://www.accessscience.com>

[1]The data used to make the map came from "A new ice thickness and subglacial topographic model of the Antarctic" prepared by the BEDMAP Consortium, which is sponsored by the European Ice Sheet Modeling Initiative, Scientific Committee on Antarctic Research.

Appendix: Published Fluxes

Published			Calculated			
Location (Glacier)	Total Area (m^2)	Sediment Flux (m^3/a)	Sediment Yield ($m^3/m^2/a$)	Total Area of GCB	Flux applied to GCB(m^3/a)	Inferred Gray GZW deposition duration (years)*
Alaska						
Caroll, Goldthwait	5.27×10^8	2.8×10^7	5.31×10^{-2}	1.81×10^{12}	9.612×10^{10}	29.1
Lituya/N Crillon	1.74×10^8	1.46×10^7	8.39×10^{-2}	1.81×10^{12}	1.518×10^{11}	18.6
Grand pac/Margerie	1.1×10^9	1.3×10^7	1.18×10^{-2}	1.81×10^{12}	2.138×10^{10}	130.4
Johns Hopkins	3.16×10^8	2.4×10^7	7.59×10^{-2}	1.81×10^{12}	1.374×10^{11}	20.4
Crillon	7.1×10^7	1.6×10^6	2.25×10^{-2}	1.81×10^{12}	4.077×10^{10}	68.4
Muir Inlet	6.83×10^8	2.06×10^7	3.02×10^{-2}	1.81×10^{12}	5.457×10^{10}	51.1
Hubbard	3.87×10^9	1×10^8	2.59×10^{-2}	1.81×10^{12}	4.681×10^{10}	59.6
Icy Bay	1.59×10^9	5×10^7	3.15×10^{-2}	1.81×10^{12}	5.704×10^{10}	48.9
McBride	1.43×10^8	2×10^6	1.40×10^{-2}	1.81×10^{12}	2.530×10^{10}	110.3
Malaspina	5.01×10^9	1×10^6	2.00×10^{-4}	1.81×10^{12}	3.613×10^8	7728

*To calculate the gray GZW duration, a sediment volume of 2.79×10^{12} m^3 was used

Published flux rates for Glaciers in Alaska as reported by Hallet et al., 1996. Corresponding yields calculated, and its application to the Glomar-Challenger-Basin (GCB) drainage area to generate duration.

Published			Calculated			
Glacier	Total Area (m^2)	Sediment Flux (m^3/yr)	Sediment Yield (m^3/m^2/a)	Total Area of GCB	Flux applied to GCB(m^3/a)	Inferred Gray GZW deposition duration (years) *
Central Asia						
Fedchenko	6.62×10^8	3.9×10^6	5.89×10^{-3}	1.81×10^{12}	1.066×10^{10}	260.7
Zaravshanskiy	1.34×10^8	9×10^5	6.72×10^{-3}	1.81×10^{12}	1.215×10^{10}	228.7
RGO	1.09×10^8	4.7×10^5	4.31×10^{-3}	1.81×10^{12}	7.801×10^9	357.7
IMAT	3.8×10^6	4.25×10^3	1.12×10^{-3}	1.81×10^{12}	2.023×10^9	1381.2
Ajutor-3	3.4×10^6	1.1×10^3	3.24×10^{-4}	1.81×10^{12}	5.853×10^8	4769.2
Karabatak	4.7×10^6	2.4×10^3	5.11×10^{-4}	1.81×10^{12}	9.238×10^8	3019.5
Other Areas						
Cambridge, Canada	6.8×10^9	1169	1.72×10^{-7}	1.81×10^{12}	3.110×10^5	9.0×10^6
Kangerdlug, Greenland	5×10^9	894	1.79×10^{-7}	1.81×10^{12}	3.235×10^5	8.6×10^6
Mikis Fjord, Greenland	1.95×10^8	14	7.18×10^{-8}	1.81×10^{12}	1.299×10^5	2.1×10^7
Nansen Fjord, Greenland	9.52×10^9	232.05	2.44×10^{-8}	1.81×10^{12}	4.411×10^4	6.3×10^7
North Sea Fan, Norway	2.5×10^{11}	8×10^8	3.2×10^{-6}	1.81×10^{12}	5.79×10^6	4.8×10^5
Antarctica						
PITIS	5×10^{11}	8×10^8	1.6×10^{-6}	1.81×10^{12}	2.896×10^6	9.6×10^5

*To calculate the gray GZW duration, a sediment volume of 2.79×10^{12} m^3 was used

Published flux rates for Glaciers and/or Fjords in Central Asia, Canada, Greenland, Norway, and Antarctica as reported by Hallet et al. (1996), Nygard et al. (2007), Graham et al. (2010). Corresponding yields calculated, and its application to the Glomar-Challenger-Basin drainage area to generate duration.

Vita

Boluwatife Owolana was born in Nigeria on October, 1985. Bolu, his parents and two siblings, moved to Philadelphia, USA, where he attended and graduated from Frankford High School in May 2002. He received a Bachelor of Science degree in biology from Neumann University in May 2007. Following his time at Neumann University, he worked in the pharmaceutical industry as an analytical chemist for two years before discovering geology and deciding to pursue a master's degree in the subject at Louisiana State University. Following graduation from LSU, Bolu plans to move to Dallas, Texas to work as a geologist for EnCana Oil & Gas (USA) Inc.